Reactive transport equations for estuarine, coastal and shelf sea modelling[1]

Eric Deleersnijder, 4-14 September 2023

Contents

Abstract 1
1. Introduction 2
2. Mass budget: a first approach 3
   2.1. Density, concentration, velocity and related concepts 3
   2.2. Mass budget of a constituent 5
   2.3. Continuity equation 8
   2.4. Conservative and convective forms 9
   2.5. Boussinesq approximation 10
3. Space and time scales of variability 11
   3.1. Variability of geophysical and environmental flows 11
   3.2. Averaging operators 12
   3.3. The averaged reactive transport equation 13
   3.4. Boundary conditions for the reactive transport equation 15
   3.5. Turbulent momentum flux 16
4. Properties of the solution of the reactive transport equation 17
   4.1. One-dimensional advection-diffusion problem 18
   4.2. Mass conservation and concentration homogenisation 19
   4.3. Behaviour of concentration extrema 21
   4.4. First-order decay and diffusion in a simple water column model 22
5. Numerical simulation 26
   5.1. Small aspect ratio flows 26
   5.2. Numerical schemes for advection, diffusion and reactions 27
   5.3. Ecological modelling 29
6. Additional remarks 29
Acknowledgements 30
References 30

Abstract. *We introduce the basic variables for tackling the mass budget of every constituent of a fluid mixture. Then, taking into account advection, molecular diffusion and reactions, we establish the conservation equation governing the constituent concentrations. We describe the space and time variability of processes taking place in estuaries, coastal regions and shelf seas, allowing us to derive the suitably-averaged reactive transport equation under the Boussinesq approximation. Some of the properties of its solutions of it are discussed. We briefly approach the related numerical aspects and*

[1] No claim is made that this study is entirely original. Instead, some of the theoretical developments in this working note are significantly inspired by de Groot and Mazur (1962) and Nihoul (1981).

give a few examples of application. Finally, we provide pieces of information about sediment dynamics, wetting and drying, and diagnostic methods.

1. Introduction

Oceans cover about 70% of the surface of the Earth. Estuaries, coastal and shelf seas represent about 8% of the ocean surface, but account for less than 1% of its volume. However, they have a key biogeochemical role. They are at the interface between land and (deep) oceans and contribute about 25% of the global ocean primary productivity (Yool and Fasham 2001). The impact of human activities cannot be overestimated: agriculture, fisheries, deforestation, damming, waste disposal, industrial pollution and shipping exert a detrimental pressure on estuaries and coastal regions (Crossland et al. 2005). This is unsurprising since about 60% of the world population lives within 60 km of the nearest coastline (Rao and Murthy 2008).

We will deal with transport processes taking place in geophysical and environmental flows, chiefly in estuaries, coastal regions and shelf seas. The driving forces of such flows are largely independent of human action. In geophysical flows, Earth's rotation is of a primary importance (e.g. Cushman-Roisin and Beckers 2011), while it is less so in environmental flows.

The processes of interest take place in a multi-constituent fluid, which consists of pure water and many other substances. The density of this fluid mixture exhibits relatively small variations, allowing us to resort to the Boussinesq approximation. The range of the relevant space and time scales is so great that it is impossible to explicitly resolve all of the processes, hence the need to parameterise (e.g. Mellor and Yamada 1992, Rodi 1993, Large et al. 1994, Burchard 2002, Umlauf and Burchard 2005) or super-parameterise (e.g. Campin et al. 2011, Hannah et al. 2020) the unresolved ones. The rotation of the Earth has no direct impact on the formulation of the mass conservation equations, as opposed to the momentum equations, in which the Coriolis force often plays a crucial role. The aspect ratio (ratio of the vertical length scale to the horizontal one) is generally small, in which case the hydrostatic approximation can be made. The water-air interface is a free boundary (hydrodynamics determines its motion), requiring specific boundary conditions to be implemented.

In Section 2, we will introduce basic variables and notions (e.g. concentration, velocity, fluid parcel, material derivative) and make a first approach to the mass budget equations. Then, the space and time scales of variability will be presented as well as the relevant averaging operators and the concept of eddy coefficient, leading to the final form of the reactive transport equation (Section 3). In Section 4, some of the properties of the solution of advection-diffusion-reaction equations will be established. Then, we will address some aspects of the numerical solution of the equations under study and give a few examples of application (Section 5). In Section 6, we provide pieces of information about sediment dynamics, wetting and drying, and diagnostic methods.

2. Mass budget: a first approach

We wish to describe processes taking place in the abovementioned water bodies. The fluid to be dealt with is a mixture of pure water (H_2O) and many other constituents. We will establish the equations governing the concentration of all the constituents of the mixture under study as well as the concentration of aggregates thereof (i.e., groups of constituents), including the concentration of the mixture itself, which, for simplicity, will sometimes be referred to as the water.

2.1. Density, concentration, velocity and related concepts

We resort to the continuous media approach, leading to the definition and manipulation of pointwise, macroscopic variables (e.g., density, concentration, velocity, salinity, etc.) that are the solutions of partial differential problems. The rationale for this choice is that the largest microscopic length scale, $\max L_{\text{micro}} \approx 10^{-9}$ m (typical order of magnitude of the distance between molecules), is much smaller than the smallest macroscopic length scale, $\min L_{\text{macro}} \approx 10^{-4}$ m ≈ Kolmogorov length scale (e.g., Section 1.2 of Batchelor 1967). Then, an elemental (control) volume is defined as a portion of the domain of interest (denoted $\delta\Omega$) whose volume δV is such that $\max L_{\text{micro}} << \delta V^{1/3} << \min L_{\text{macro}}$. Such a volume appears to be "infinitely small" from the macroscopic vantage point, and "infinitely large" from the microscopic one. All the pointwise variables introduced hereinafter are associated with elemental volumes. They will be manipulated with the help of the tools of mathematical analysis (limits, derivatives, integrals).

We assume that the mixture under study consists of $N+1$ constituents. Each of them will be identified by subscript n, with $n=0$ for pure water and $n \in [1,N]$ for the other components of the fluid mixture. The latter (dissolved gases, pollutants, nutrients, sediments particles, plankton cells, etc.) are considered to be in dissolved (resp. particulate) form if their size is smaller (resp. greater) than 5×10^{-7} m (e.g. Baretta-Bekker et al. 1998). Obviously, this distinction is somewhat arbitrary.

At time t, we consider the elemental control volume $\delta\Omega$ (whose volume is δV) located at $\mathbf{x} = x\,\mathbf{e}_x + y\,\mathbf{e}_y + z\,\mathbf{e}_z$, where x, y and z are Cartesian coordinates[2], whilst $\mathbf{e}_x$, $\mathbf{e}_y$ and $\mathbf{e}_z$ are the associated basis vectors, whose norms are equal to unity. The density $\rho_n(t,\mathbf{x})$ of the n-th constituent (n=0,1,2,... N) is $\delta m_n / \delta V$, where δm_n denotes the mass of the n-th constituent contained in the elemental control volume. Obviously, the physical dimension of the density is density $\text{mass}\times\text{length}^{-3}$. Then, the density of the mixture is $\rho = (\rho_0 + \rho_1 + ... \rho_N) / \delta V$. The concentration of the n-th constituent is defined as dimensionless ratio $C_n(t,\mathbf{x}) = \rho_n(t,\mathbf{x}) / \rho(t,\mathbf{x})$. Clearly, every concentration is such that $0 \le C_n(t,\mathbf{x}) \le 1$ and the sum of all the concentrations is equal to unity (e.g., Nihoul 1981)

$$\sum_{n=0}^{N} C_n(t,\mathbf{x}) = \sum_{n=0}^{N} \frac{\rho_n(t,\mathbf{x})}{\rho(t,\mathbf{x})} = 1 \qquad (1)$$

The concentrations, as introduced above, are often referred to as mass fractions. Many other definitions may be contemplated. They must be tackled with great care. Failing to do so

[2] As is common practice in marine modelling, x and y are assumed to be horizontal coordinates, and z is the vertical coordinate, increasing upwards.

may lead to misconceptions. Transforming one type of concentration into another is no insuperable task. However, to every definition of the concentration corresponds a specific formulation of the equation governing the evolution of such a variable (e.g. de Groot and Mazur 1962).

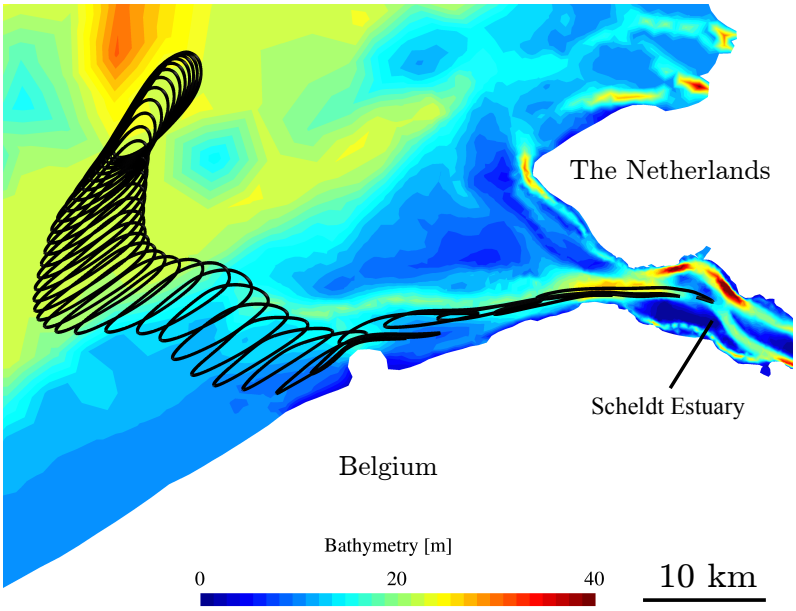


Figure 1. Numerical simulation performed over a period of 30 days of the trajectory of a fluid parcel initially located near the mouth of the Scheldt Estuary. The near-ellipses are due to dominant tidal component (M2), whose period is approximately 12 hours and 25 minutes. Long term and distance transport takes place at a velocity (Lagrangian residual velocity) much slower than that directly related to tidal motion. The numerical results and the figure are due to Benjamin de Brye, who used SLIM (www.slim-ocean.be).

The velocity of the n-th constituent, $\mathbf{v}_n(t,\mathbf{x})$, is defined as the arithmetic mean of the velocities of the particles of this constituent that are at time t in control volume $\delta\Omega$. The velocity of the mixture (which will also be termed "fluid velocity" or "water velocity"), $\mathbf{v}(t,\mathbf{x}) = u(t,\mathbf{x})\mathbf{e}_x + v(t,\mathbf{x})\mathbf{e}_y + w(t,\mathbf{x})\mathbf{e}_z$, is defined to be the mass-weighted average of the velocities of the particles (atoms, molecules, ions) of all the constituents, yielding

$$\mathbf{v} = \frac{1}{\rho}\sum_{n=0}^{N}\rho_n\mathbf{v}_n = \sum_{n=0}^{N}C_n\mathbf{v}_n \tag{2}$$

A fluid parcel is a moving elemental volume whose velocity is that of the fluid mixture. This velocity is usually termed "barycentric velocity", for it may be seen to be equal to the velocity of the centre of mass of the particles present in the fluid parcel. A fluid parcel does not always contain the same particles[3] but, as will be seen below, its mass remains constant.

[3] To grasp the distinction between the concept of fluid parcel and that of (constituent) particle, see, e.g., Deleersnijder (2020), and Section 1.2.1 of Lucas and Deleersnijder (2020).

The position vector $\mathbf{r}(t)$ of a fluid parcel is the solution of the differential problem

$$\begin{cases} \dfrac{d}{dt}\mathbf{r}(t) \;=\; \mathbf{v}[t,\mathbf{r}(t)] \\ \mathbf{r}(0) \;=\; \mathbf{r}_0 \end{cases} \tag{3}$$

Solving analytically (3) is hardly ever possible, for this problem is generally non-linear. In most cases, only a numerical approximation to the solution may be constructed, which may point to important properties of the flow under study as is illustrated in Figure 1.

The material derivative is the time rate of change measured by an observer "tied" to a fluid parcel. Accordingly, the material derivative of function $\varsigma(t,\mathbf{x})$ is

$$D_t\,\varsigma(t,\mathbf{x}) \;=\; \frac{d}{dt}\varsigma[t,\mathbf{r}(t)] = \left[\frac{\partial\varsigma}{\partial t} + \frac{d\mathbf{r}}{dt}\bullet\nabla\varsigma\right]_{\mathbf{x}=\mathbf{r}(t)} \;=\; \underbrace{\left[\frac{\partial}{\partial t} + \mathbf{v}(t,\mathbf{x})\bullet\nabla\right]}_{=D_t}\varsigma(t,\mathbf{x}) \tag{4}$$

where $\nabla = \mathbf{e}_x\,\partial/\partial x + \mathbf{e}_y\,\partial/\partial y + \mathbf{e}_z\,\partial/\partial z$ is the del operator. The material derivative is a Lagrangian concept (it is related to a fluid parcel) expressed in Eulerian terms (it involves partial derivatives in time and space). Interestingly, the identity $D_t\,\mathbf{x} = \mathbf{v}(t,\mathbf{x})$ is readily seen to hold valid. Furthermore, the material derivative of a time-independent (or steady-state) function, $D_t\,\varsigma(\mathbf{x}) = \mathbf{v}\bullet\nabla\varsigma(\mathbf{x})$, is zero if and only if the fluid motion follows the isolines of this function.

2.2. Mass budget of a constituent

Consider finite-sized motionless control volume Ω delimited by surface Γ, whose outward unit vector is $\mathbf{n}$ (Figure 2). The mass $m_n(t)$ of the n-th constituent contained in this control volume evolves under the influence of reactions (i.e., production and destruction) and transport (i.e., particle motion) through boundary Γ, yielding the following generic expression

$$m_n(t+\delta t) \;=\; m_n(t) \;+\; (\text{mass produced by reactions}) \;-\; (\text{outgoing mass through } \Gamma) \tag{5}$$

where δt denotes a suitable time increment.

In accordance with the above definitions of the density and concentration, the mass of the n-th constituent contained in elemental control volume $\delta\Omega \subset \Omega$ is $\delta m_n = \rho_n \delta V = \rho C_n \delta V$. Thus, the mass of this constituent present in Ω is the sum of the elemental masses:

$$m_n \;=\; \sum_{\mathbf{x}\in\Omega} \rho C_n\,\delta V \;=\; \int_{\Omega} \rho C_n\,d\Omega \tag{6}$$

The mass produced during time interval $[t,t+\delta t]$ is $\rho\theta_n\,\delta V\,\delta t$ in the limit $\delta t \to 0$, where $\theta_n(t,\mathbf{x})$ is the local net production (i.e., production – destruction) rate of the constituent under consideration. Its physical dimension is $(\text{time})^{-1}$. For the whole control volume, one obtains

$$\text{mass produced by reactions} \;\sim\; \sum_{\mathbf{x}\in\Omega} \rho\theta_n\,\delta V\,\delta t \;\sim\; \int_{\Omega} \rho\theta_n\,d\Omega\,\delta t \quad,\quad \delta t \to 0 \tag{7}$$

The net production rate may take several forms. For the decay of a radioactive constituent (nuclear reaction), the relevant expression is $\theta_n = -C_n/\tau_n$, where constant τ_n is the mean life of the constituent. The mean lives vary over a wide range of orders of magnitude. For example, the mean lives of carbon-14, caesium-137, strontium-90 and iodine-131 are

approximately equal to 8,300 years, 43 years, 41 years and 12 days, respectively. The mean life should not be mistaken for the half-life (time needed for half of the atoms to decay), which is $\tau_{n,1/2} = (\log 2) \times \tau_n \approx 0.7 \times \tau_n$. An expression similar to the rate of decay of a radionuclide is also used for representing in an approximate way the destruction of many types of constituents even though the reaction involved is not of a nuclear nature. This is referred to as a first-order process. Other reactive processes must also to be considered, which are of a chemical or biological nature. For instance, for predation, if *m*-th and *n*-th constituents are related to the predator and the prey, respectively, then the corresponding reaction terms read $\theta_m = C_m C_n / \tau_{m,n}$ and $\theta_n = -C_m C_n / \tau_{m,n}$ where the timescale $\tau_{m,n}$ generally is an intricate function of the concentrations C_m and C_n, temperature, etc. A constituent whose net production rate is zero at any time and location ($\theta_n = 0$) is termed passive or inert. For example, pure water (devoid of tritiated water) is a passive constituent and dissolved CFC (chlorofluorocarbon) gases are almost passive in the aquatic environment — though they contribute to ozone depletion ("ozone hole") in the stratosphere.

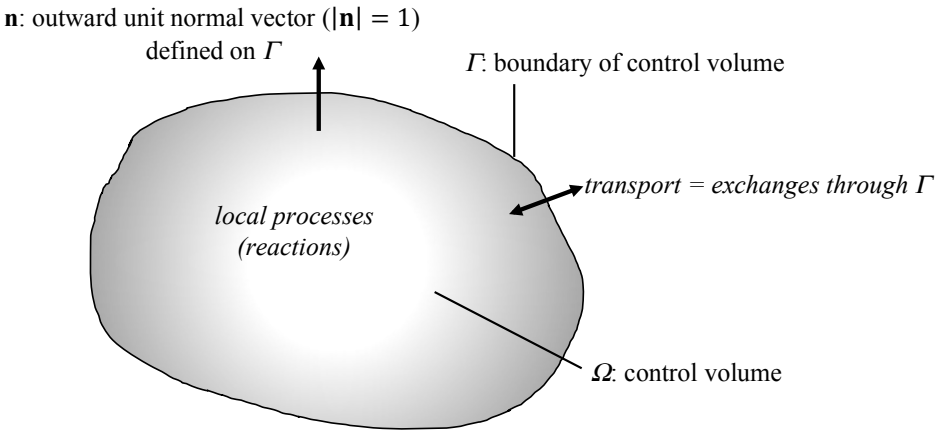


Figure 2. Illustration of control volume Ω delimited by surface Γ. A control volume is a volume delineated by thought whose mass budget is to be examined. The mass of every constituent contained in Ω is impacted by reactions (i.e. local phenomena that are not directly related to motion) and exchanges through Γ (transport processes).

At any time and location in the mixture under study, there is neither net creation of matter nor net destruction of it, implying that

$$\sum_{n=0}^{N} \theta_n = 0 \tag{8}$$

In other words, according to the famous aphorism generally attributed to French chemist Antoine Laurent Lavoisier (1743-1794), "nothing is lost, nothing is created, everything is transformed" (*rien ne se perd, rien ne se crée, tout se transforme*).

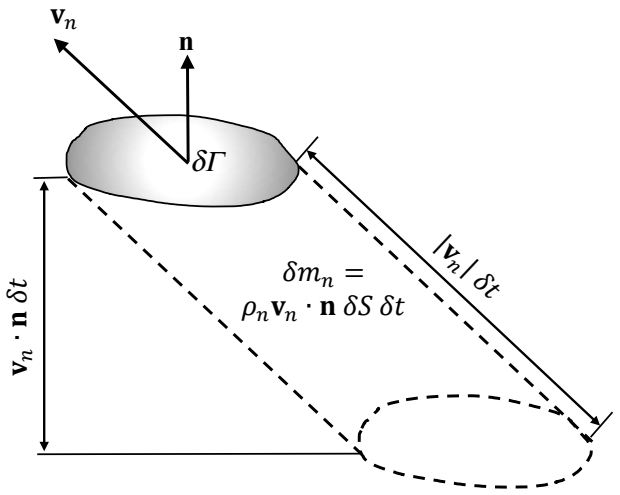


Figure 3. Schematic helping to evaluate δm_n, the mass of the n-th constituent leaving the domain of interest through boundary element $\delta\Gamma$ during time interval $[t, t+\delta t]$, with $\delta t \to 0$.

As may be seen in Figure 3, the mass of the n-th constituent leaving ($\mathbf{v}_n \bullet \mathbf{n} > 0$) the control volume during the time interval $[t, t+\delta t]$, with $\delta t \to 0$, through boundary element $\delta\Gamma$ tends to $\rho_n \mathbf{v}_n \bullet \mathbf{n}\,\delta S\,\delta t$, where δS is the area of $\delta\Gamma$. This expression still holds valid if the n-th constituent actually enters the control volume rather than leaving it ($\mathbf{v}_n \bullet \mathbf{n} < 0$). Then, the net outgoing mass reads

$$\text{outgoing mass through } \Gamma \;\sim\; \sum_{\mathbf{x}\in\Gamma} \rho_n \mathbf{v}_n \bullet \mathbf{n}\,\delta S\,\delta t \;\sim\; \int_{\Gamma} \rho_n \mathbf{v}_n \bullet \mathbf{n}\,d\Gamma\,\delta t \quad , \quad \delta t \to 0 \tag{9}$$

Combining (5), (7) and (9), we obtain asymptotic expression

$$\frac{m_n(t+\delta t) - m_n(t)}{\delta t} \;\sim\; \int_{\Omega} \rho\theta_n\,d\Omega \;-\; \int_{\Gamma} \rho_n \mathbf{v}_n \bullet \mathbf{n}\,d\Gamma \quad , \quad \delta t \to 0 \tag{10}$$

which, in the limit $\delta t \to 0$, yields

$$\lim_{\delta t\to 0} \frac{m_n(t+\delta t) - m_n(t)}{\delta t} \;=\; \frac{dm_n}{dt} \;=\; \int_{\Omega} \rho\theta_n\,d\Omega \;-\; \int_{\Gamma} \rho_n \mathbf{v}_n \bullet \mathbf{n}\,d\Gamma \tag{11}$$

Using (6) and the divergence theorem allows transforming (11) to

$$\frac{d}{dt}\int_{\Omega} \rho C_n\,d\Omega \;=\; \int_{\Omega} \left[\rho\theta_n - \nabla \bullet (\rho C_n \mathbf{v}_n)\right] d\Omega \tag{12}$$

Since control domain Ω is fixed (motionless), the following relation holds valid

$$\frac{d}{dt}\int_{\Omega} \rho C_n\,d\Omega \;=\; \int_{\Omega} \frac{\partial}{\partial t}(\rho C_n)\,d\Omega \tag{13}$$

Substituting (13) into (12) leads to

$$\int_{\Omega} \frac{\partial}{\partial t}(\rho C_n)\,d\Omega \;=\; \int_{\Omega} \left[\rho\theta_n - \nabla \bullet (\rho C_n \mathbf{v}_n)\right] d\Omega \tag{14}$$

This integral expression must hold true for any control volume Ω. This is why the integrand in the left-hand side of (14) must be equal to that of the right-hand side, yielding the following partial differential equation

$$\frac{\partial}{\partial t}(\rho C_n) = \rho\theta_n - \nabla\bullet(\rho C_n \mathbf{v}_n) \tag{15}$$

This relation, which is often called "reactive transport equation", governs the evolution of the concentration of the *n*-th constituent. Obviously, similar equations are applicable to all the constituents of the fluid mixture under study. It was established from an "accounting exercise", consisting in evaluating, during an elemental time interval, the mass of the constituent under study crossing the boundary of the control volume (transport processes) and the mass being produced or destroyed inside the control volume (reactive phenomena).

In (15), the product $\rho C_n \mathbf{v}_n$ is the mass flux of the *n*-th constituent. Its physical dimension is readily seen to be $\text{mass}\times\text{length}^{-2}\times\text{time}^{-1}$. Unfortunately, the word "flux" may have various meanings and, hence, may refer to quantities with different physical dimensions.

2.3. Continuity equation

The fluid mixture we wish to study is made up of so large a number of constituents that it s probably impossible to study each of them individually. Therefore, it is appropriate to deal with groups of constituents, which we will call aggregates (e.g., Nihoul 1993). The concentration C_{ag} and velocity $\mathbf{v}_{ag}$ of an aggregate are $C_{ag} = \upsilon_0 C_0 + \upsilon_1 C_1 + ... \upsilon_N C_N$ and $\mathbf{v}_{ag} = (\upsilon_0 C_0 \mathbf{v}_0 + \upsilon_1 C_1 \mathbf{v}_1 + ... \upsilon_N C_N \mathbf{v}_N)/C_{ag}$, where υ_n is equal to unity or zero according to whether the *n*-th constituent is part of the aggregate under consideration or not. Then, concentration C_{ag} is readily seen to obey equation

$$\frac{\partial}{\partial t}(\rho C_{ag}) = \rho \sum_{n=0}^{N} \upsilon_n \theta_n - \nabla\bullet(\rho C_{ag}\mathbf{v}_{ag}) \quad , \tag{16}$$

which is obtained by taking the sum of (15) over the relevant concentrations. For instance, salinity is the concentration, often denoted $S(t,\mathbf{x})$, of the dissolved constituents that are collectively referred to as salt, i.e. sodium chloride, magnesium sulphate, potassium nitrate, etc. Salt is regarded as a passive aggregate: its net production-destruction rate is assumed to be zero. For most of the applications mentioned above, salinity ranges from approximately zero (freshwater) to 40×10^{-3} (typical value of the salinity in the Red Sea). The average seawater salinity is $\approx 35\times10^{-3}$. For evaluating salinity from *in situ* data, it is assumed that water consists of only pure water and salt (Feistel 2008), for the concentrations of the other constituents is generally very small.

The equation obeyed by the concentration of an aggregate has the same form as that governing the equation of an individual constituent. Therefore, there is no need to keep distinguishing aggregates for individual constituents. Accordingly, for simplicity, we will only use the term "constituent" from here on even if the substance under consideration actually is an aggregate.

The fluid mixture is the aggregate encompassing all the constituents. Its concentration is identically equal to unity. Taking the sum of (15) over all the constituents yields

$$\frac{\partial}{\partial t}(\rho \underbrace{\sum_{n=0}^{N} C_n}_{=1,\text{ see (1)}}) = \rho \underbrace{\sum_{n=0}^{N} \theta_n}_{=0,\text{ see (8)}} - \nabla\bullet(\underbrace{\rho \sum_{n=0}^{N} C_n \mathbf{v}_n}_{\rho\mathbf{v},\text{ see (2)}}) \tag{17}$$

which simplifies to

$$\frac{\partial \rho}{\partial t} = \nabla\bullet(\rho\mathbf{v}) \tag{18}$$

This is the mass conservation equation for the fluid mixture, which is usually called "continuity equation". The form of this relation is similar to that valid for a fluid consisting of a single constituent. This is essentially due to the use of the barycentric velocity.

Continuity equation (18) can be rewritten a follows:

$$D_t\rho = -\rho\,\nabla\bullet\mathbf{v} \quad . \tag{19}$$

Thus, unsurprisingly, the density of a fluid parcel decreases (resp. increases) if $\nabla\bullet\mathbf{v}$, the divergence of the mixture velocity, is positive (resp. negative).

2.4. Conservative and convective forms

Velocity $\mathbf{v}_n$ appearing in (15) can be neither measured nor modelled easily in the framework of continuous media theory, rendering this equation rather useless for practical purposes. As will be seen, it is convenient to rewrite $\mathbf{v}_n$ as follows:

$$\mathbf{v}_n = \mathbf{v} + (\mathbf{v}_n - \mathbf{v}) \tag{20}$$

where $\mathbf{v}$ is the macroscopic velocity of the fluid mixture, which is the velocity that is (approximately) measured by most instruments, whilst $\mathbf{v}_n - \mathbf{v}$ is due to microscopic-scale processes, the details of which cannot be resolved (i.e., modelled explicitly) in the approach adopted herein. As a result, flux $\rho C_n \mathbf{v}_n$ may be split into two contributions,

$$\rho C_n \mathbf{v}_n = \rho C_n \mathbf{v} + \underbrace{\rho C_n (\mathbf{v}_n - \mathbf{v})}_{=\rho\mathbf{q}_n} \quad , \tag{21}$$

where $\rho C_n \mathbf{v}$ is the resolved mass flux (associated with macroscopic-scale processes), which is usually referred to as the advective mass flux, and $\rho\mathbf{q}_n$ is the macroscopic-scale mass flux due to unresolved, microscopic-scale processes. Fluxes $\mathbf{q}_n$ satisfy

$$\sum_{n=0}^{N} \rho\mathbf{q}_n = \sum_{n=0}^{N} \rho C_n (\mathbf{v}_n - \mathbf{v}) = \underbrace{\sum_{n=0}^{N} \rho C_n \mathbf{v}_n}_{=\rho\mathbf{v},\text{ see (2)}} - \underbrace{\sum_{n=0}^{N} \rho C_n \mathbf{v}}_{=\rho\mathbf{v},\text{ see (1)}} = 0 \tag{22}$$

If there are only two constituents (N=1), the unresolved fluxes are associated with molecular diffusion and are parameterised by means of Fick's law (Fick 1855): $\rho\mathbf{q}_1 = -\rho\kappa\nabla C_1$ and $\rho\mathbf{q}_2 = -\rho\kappa\nabla C_2$, where κ ($\mathrm{m^2\,s^{-1}}$) is the molecular diffusivity. These down-gradient mass fluxes tend to homogenise the related concentrations. If $N > 1$, the expression of the molecular fluxes can be much more intricate (e.g., Jou et al. 1996).

Substituting (21) into (15) yields

$$\frac{\partial}{\partial t}(\rho C_n) = \rho\theta_n - \nabla\bullet(\rho C_n \mathbf{v} + \rho\mathbf{q}_n) \tag{23}$$

which is a conservative form of the advection-diffusion-reaction equation. This relation is said to be "conservative" since it has been obtained from mass conservation or mass budget

considerations. Combining (18) and (23) and using definition (4) of the material derivative allows transforming (23) into the associated convective form:

$$D_t C_n \;=\; \theta_n \;-\; \frac{1}{\rho}\nabla\bullet(\rho\mathbf{q}_n) \quad . \tag{24}$$

Thus, the rate of change of the concentration measured by an observer "tied" to a fluid parcel depends on the reactions and the microscopic processes, but not on the compressibility of the fluid. In other words, the concentration of a constituent defined as a mass fraction is not directly impacted by the modification of the density of the fluid mixture. Obviously, this does not apply to the density of a constituent. Indeed, the material derivative of the density of a constituent obeys $D_t\rho_n = \rho_n D_t\rho/\rho + \rho\theta_n - \nabla\bullet(\rho\mathbf{q}_n)$.

2.5. Boussinesq approximation

In the aquatic environment, pure water is, by far, the dominant constituent. Therefore, the density of any mixture is close to that of pure water, ρ_0. In fact, the density obeys

$$1{,}000\ \mathrm{kg\ m^{-3}} \;\lesssim\; \rho \;\lesssim\; 1{,}050\ \mathrm{kg\ m^{-3}} \quad . \tag{25}$$

In most of the flows of interest, the range of variation of the density actually is much smaller than that suggested in this formula. The value of the density is obtained from the equation of state (e.g., Feistel 2008), which stipulates that it depends on the temperature and the salinity. The impact of the pressure variations is generally ignored as long as the order of magnitude of the height of the water column does not exceed a few hundreds of metres.

The smallness of the range of variation of the density will allow us to simplify the mass budget equations derived above: we will estimate the order of magnitude of the terms of these equations and disregard the smallest ones. Performing such a scaling (or any other scaling) is not as straightforward as we might believe at the first glance (e.g., Deleersnijder 2019a).

Let $\rho_\bullet$, $\Delta\rho$, V denote an appropriate reference value of the density, the order of magnitude of its variations and a relevant velocity scale, respectively. Further assume that T and L are relevant time- and space-scales of the flow under consideration. Then, the following dimensionless variables and differential operators (identified by primes) may be introduced

$$\frac{\partial}{\partial t} = \frac{1}{T}\frac{\partial}{\partial t'}\ ,\quad \nabla = \frac{1}{L}\nabla'\ ,\quad \rho = \rho_\bullet + \Delta\rho\,\rho'\ ,\quad \mathbf{v} = V\,\mathbf{v}' \quad . \tag{26}$$

with $\Delta\rho/\rho_\bullet << 1$. This constraint is the key (necessary) condition for introducing simplifications in the governing equations that are commonly referred to as the Boussinesq approximation. A detailed discussion of the latter may be found in Section 4.9 of Kundu et al. (2012).

Substituting the dimensionless variables into continuity equation (18) leads to

$$\frac{L}{VT}\frac{\Delta\rho}{\rho_\bullet}\frac{\partial\rho'}{\partial t'} \;+\; \frac{\Delta\rho}{\rho_\bullet}\mathbf{v}'\bullet\nabla'\rho' \;+\; \left(1+\frac{\Delta\rho}{\rho_\bullet}\rho'\right)\nabla'\bullet\mathbf{v}' \;=\; 0 \quad . \tag{27}$$

Since it is assumed that $\Delta\rho/\rho_\bullet << 1$, dimensionless continuity equation (27) may be simplified to $\nabla'\bullet\mathbf{v}' = 0$, which is equivalent to (in dimensional variables)

$$\nabla\bullet\mathbf{v} \;=\; 0 \tag{28}$$

or, equivalently, $\partial u/\partial x + \partial v/\partial y + \partial w/\partial z = 0$. Simplified continuity equation (28) does not

support acoustic waves. Their frequency is sufficiently high that the dimensionless ratio $(L\,\Delta\rho)/(VT\,\rho_\bullet)$ is of order unity, implying that the relevant continuity equation must include $\partial\rho/\partial t$ (e.g., Lighthill 1978).

Under the Boussinesq approximation, the mass of the mixture and that of the n-th constituent contained in finite-sized control volume Ω are to be estimated from the following approximations:

$$m(t) = \int_{\Omega} \rho(t,\mathbf{x})\, d\Omega \approx \rho_\bullet \int_{\Omega} d\Omega \approx \rho_\bullet V \tag{29}$$

and

$$m_n(t) = \int_{\Omega} \rho(t,\mathbf{x}) C_n(t,\mathbf{x})\, d\Omega \approx \rho_\bullet \int_{\Omega} C_n(t,\mathbf{x})\, d\Omega \tag{30}$$

where V is the volume of Ω. By the same token, the conservative and convective reactive transport equations (23) and (24) transform to

$$\frac{\partial C_n}{\partial t} = \theta_n - \nabla\bullet(C_n\mathbf{v} + \mathbf{q}_n) \tag{31}$$

and

$$D_t C_n = \theta_n - \nabla\bullet\mathbf{q}_n \tag{32}$$

From here on, the Boussinesq approximation will be assumed to be in effect.

3. Space and time scales of variability

In the developments above, the microscopic-scales were not dealt with explicitly (though we made it clear that their impact on macroscopic scales has to be taken into account) and the macroscopic scales were explicitly represented in the framework of the continuous media approach. Unfortunately, the range of the space and time scales over which the macroscopic processes take place is so great that only a fraction of them can be modelled explicitly: we will resolve the larger scales and filter out the smaller ones.

3.1. Variability of geophysical and environmental flows

It is generally believed that Leonardo da Vinci (1452-1519) (e.g. Frisch 1995) was the first to realise that many fluid flows exhibit a wide range of space and time scales of motion. However, it is Irish scientist Osborne Reynolds (1842-1912) who first performed laboratory experiments and theoretical developments on this topic. Reynolds (1883) injected dye into a fluid flowing in a pipe. He showed that there exist two radically different types of flows, the laminar flows and the turbulent ones. The seemingly erratic turbulent motions, which are of a macroscopic nature, generally lead to mixing that is much more efficient than that caused by microscopic-scale processes (molecular diffusion).

Reynolds suggested that the key parameters of his experiment are the cross-section averaged velocity U, the pipe's diameter D and the kinematic viscosity of the fluid ν ($\mathrm{m^2\,s^{-1}}$). He combined them to form dimensionless expression $Re = UD/\nu$, which is nowadays called "Reynolds number". For small (resp. large) values of the latter, the flow is laminar (resp. turbulent). It is at $Re \approx 3\times10^3$ that the transition occurs.

Turbulent flows are always rotational and unsteady; they exhibit a wide range of time and space scales of motion (e.g., Ferziger 2005). In some idealised situations, the ratio of the largest length scale to the smallest one is of order $Re^{3/4}$; in general, this ratio is an increasing function of Re . Needless to say, the Reynolds numbers of the flows dealt with herein is much larger than those generally associated with pipe flows. Assume that the typical velocity, length scale and order of magnitude of the kinematic viscosity are $1\,\mathrm{m\,s^{-1}}$, 10^2 m and $10^{-6}\ \mathrm{m^2\,s^{-1}}$, respectively. These values are appropriate for many estuarine flows. They lead to $Re \approx 10^8$, which is presumably a lower bound of the Reynolds number for the flows we are dealing with.

Marine and oceanic flows are more complex that those occurring in a pipe inasmuch as they encompass a much wider range of processes. Several attempts have been made to name (some of) them as well as delineate schematically their time and space scales. See, for instance, Figure 1-1 of Cushman-Roisin (1989), Nihoul (1991, pages 39-41), Figure 2.6 of von Storch (2001), Figure 2.a of Dickey (2003), Figure 14 of Wolanski et al. (2003) or Table 1.2 of Cushman-Roisin and Beckers (2011).

Some phenomena may be worth mentioning explicitly. Micro-turbulence, with time and space scales of order $10^0 - 10^2$ s and $10^{-2} - 10^0$ m , is the phenomenon whose nature is closest to what Reynolds observed. Internal waves and turbulence generated by the breaking of the shorter of them have typical timescales of $10^2 - 10^3$ s . The corresponding horizontal length scales are $10^1 - 10^4$ m , whilst the vertical length scales do not exceed about 10^2 m . Inertial oscillations and tides exhibit a small aspect ratio (ratio of the vertical length scale to the horizontal one). Their characteristic times and horizontal lengths are of order $10^4 - 10^5$ s and $10^3 - 10^5$ m , respectively. It is also worth mentioning coastal upwelling and fronts, whose typical time and horizontal length scales are $10^5 - 10^6$ s and $10^3 - 10^4$ m . The aforementioned phenomena are such that the larger their timescale, the larger their horizontal space scale, the vertical length scale being capped by the height of the water column.

We will now outline a strategy for filtering out the smallest scales of motion.

3.2. Averaging operators

Reynolds (1895) suggested using an averaging operator in order to separate the large-scale variables, which are explicitly resolved, from the smaller-scale, unresolved ones. Accordingly, at any time and position, every variable may be viewed as the sum of two contributions $\varsigma(t,\mathbf{x}) = \overline{\varsigma}(t,\mathbf{x}) + \tilde{\varsigma}(t,\mathbf{x})$, where $\overline{\varsigma}(t,\mathbf{x})$ is the mean part of $\varsigma(t,\mathbf{x})$, while $\tilde{\varsigma}(t,\mathbf{x})$ denotes the unresolved one, with $\overline{\tilde{\varsigma}}(t,\mathbf{x}) = 0$. We must apply the averaging operator to all of the governing equations so as to derive the equations obeyed by the large-scale variables. This is, however, far from straightforward.

We might conceive time, space or ensemble averages. At a given time and position, the ensemble mean is the arithmetic mean taken over all the realisations of flows that are identical at the resolved scales. For flows that can be reproduced as many times as needed (e.g. in a flume), the ensemble average is (at least in principle) the most suitable option. However, for systems that cannot be controlled (e.g., naturally-occurring flows), ensemble means cannot be estimated. Space averages are generally difficult to estimate with currently available sensors, for the space resolution of their measurements is not sufficient. Thus, we must turn to time

averages.

The simplest temporal filter is the running mean (Germano 1992)

$$\overline{\varsigma}(t,\mathbf{x}) \;=\; \frac{1}{T}\int_{t-T/2}^{t+T/2} \varsigma(t',\mathbf{x})\,dt' \tag{33}$$

The processes whose timescales are much larger than T are hardly affected by this operator and, hence, are those that are explicitly resolved. Most sensors have a sampling frequency sufficiently high for a wide range of time averages to be performed easily. The operator must be applied to the reactive transport equations so as to obtain expressions governing the evolution of filtered concentrations. Then, it is readily seen that one of the deficiencies of running mean (33) is that it does not commute with the time derivative

$$\overline{\left(\frac{\partial \varsigma}{\partial t}\right)} \;\neq\; \frac{\partial}{\partial t}\left(\overline{\varsigma}\right) \tag{34}$$

If there were a clear separation between the timescales of the resolved and unresolved motions, then running mean (33) would commute approximately with the time derivative. Every type of operator is plagued by a number of problems to which no entirely satisfactory solution exists (e.g. Bedford et al. 1987, Stull 1988). In order to obtain tractable equations, the averaging operator should satisfy the following properties (e.g. Stull 1988):

$$\overline{\overline{\varsigma}} = \overline{\varsigma}\;,\quad \overline{\overline{\varsigma}\upsilon} = \overline{\varsigma}\,\overline{\upsilon}\;,\quad \overline{\varsigma+\upsilon} = \overline{\varsigma}+\overline{\upsilon}\;,\quad \overline{\frac{\partial \varsigma}{\partial t}} = \frac{\partial \overline{\varsigma}}{\partial t}\;,\quad \overline{\nabla \varsigma} = \nabla \overline{\varsigma} \tag{35}$$

3.3. The averaged reactive transport equation

There is no averaging operator that can be used in practice that satisfies all of the properties (35). It is, however, possible to set up an averaging strategy that meets them to an acceptable degree of accuracy.

Applying a suitable averaging to the Boussinesq version of reactive transport equation (31) yields

$$\overline{\frac{\partial C_n}{\partial t}} \;=\; \overline{\theta}_n \;-\; \overline{\nabla\bullet(C_n\mathbf{v}+\mathbf{q}_n)} \tag{36}$$

or, equivalently,

$$\overline{\frac{\partial(\overline{C}_n+\tilde{C}_n)}{\partial t}} \;=\; \overline{\overline{\theta}_n+\tilde{\theta}_n} \;-\; \overline{\nabla\bullet[(\overline{C}_n+\tilde{C}_n)(\overline{\mathbf{v}}+\tilde{\mathbf{v}})+\overline{\mathbf{q}}_n+\tilde{\mathbf{q}}_n]} \tag{37}$$

Then, by using (35), we obtain

$$\frac{\partial(\overline{C}_n+\overline{\tilde{C}}_n)}{\partial t} \;=\; \overline{\theta}_n \;+\; \overline{\tilde{\theta}}_n \;-\; \nabla\bullet(\overline{\overline{C}_n\overline{\mathbf{v}}}+\overline{\tilde{C}_n\overline{\mathbf{v}}}+\overline{\overline{C}_n\tilde{\mathbf{v}}}+\overline{\tilde{C}_n\tilde{\mathbf{v}}}+\overline{\overline{\mathbf{q}}}_n+\overline{\tilde{\mathbf{q}}}_n) \tag{38}$$

which simplifies to

$$\frac{\partial \overline{C}_n}{\partial t} \;=\; \overline{\theta}_n \;-\; \nabla\bullet(\overline{C}_n\overline{\mathbf{v}}+\overline{\tilde{C}_n\tilde{\mathbf{v}}}+\overline{\mathbf{q}}_n) \tag{39}$$

It must be underscored that most of the operations involved in the transformation of (36) to (39) are not straightforward. We repeatedly used (35) to obtain, for instance, the following results: $\overline{\overline{C}}_n = \overline{C}_n$, $\overline{\overline{C}_n\overline{\mathbf{v}}} = \overline{\overline{C}}_n\overline{\overline{\mathbf{v}}} = \overline{C}_n\overline{\mathbf{v}}$ or $\overline{\tilde{C}_n\overline{\mathbf{v}}} = \overline{\tilde{C}}_n\overline{\overline{\mathbf{v}}} = \overline{\tilde{C}}_n\overline{\mathbf{v}} = 0$. Production-destruction term θ_n

is often nonlinear. Therefore, working out a suitable averaged version of it is often delicate and, hence, has to be achieved on a case-by-case basis.

Equation (39) exhibits only averaged variables, with the noticeable exception of the advective flux $\overline{\tilde{C}_n\tilde{\mathbf{v}}}$ that is associated with unresolved (i.e., "turbulent") processes. This flux represents the impact on the resolved scales of the transport occurring at the macroscopic, unresolved scales. In order to close filtered equation (39), the flux $\overline{\tilde{C}_n\tilde{\mathbf{v}}}$ must be parameterised by having recourse to resolved variables. Flux $\overline{\tilde{C}_n\tilde{\mathbf{v}}}$ often tends to homogenise the mean concentration. This is why it is usually parameterised à la Fourier-Fick by having recourse to the so-called eddy or turbulent diffusivity κ_t :

$$\overline{\tilde{C}_n\tilde{\mathbf{v}}} \;=\; -\kappa_t \nabla \overline{C}_n \tag{40}$$

Boussinesq (1877) paved the way that led to Fourier-Fick parameterisations of unresolved macroscopic fluxes — of mass or momentum. Owing to their local nature, such expressions have been subject to much criticism since their inception. For instance, Batchelor and Townsend (1956) wrote that "Turbulent diffusion is a non local effect [...], and a description of the diffusion by some kind of integral equation is more to be expected". Deleersnijder (2019b) shows that parameterisation (40) cannot reproduce the correct shape of a seemingly simple, steady-state plume of tracer emitted by a point source unless a somewhat convoluted expression of the eddy coefficient is resorted to. Clearly, alternative approaches are needed. They are being worked out (e.g., Cushman-Roisin 2008, 2022), but they are presumably not yet sufficiently mature to be used in today's general-purpose numerical models.

Another drawback of Fourier-Fick parameterisations is related to the techniques for estimating the value of the eddy coefficients, i.e., the turbulence closure schemes. Many such methods have been worked out over the last century, but none of them was found to be universally acceptable. Most of them require the solution of additional partial differential equations (e.g., Mellor and Yamada 1982, Rodi 1993, Burchard 2002, Umlauf and Burchard 2003, Baumert et al. 2005, Umlauf and Burchard 2005, Canuto et al. 2010), which include further parameterisations that are thought by some to be, at best, questionable (e.g. Deleersnijder et al. 2008).

As opposed to the molecular diffusivity, the eddy coefficient is not a property of the constituent under consideration and the mixture it belongs to. Instead, it chiefly depends on the flow field, which is why the turbulent diffusivity is generally taken to be identical for all the constituents. Another striking difference between the eddy diffusivity and the molecular diffusivity is that the former may vary over several orders of magnitude in the same domain of interest. In the aquatic environment, typical values are such that

$$10^{-5}\ \mathrm{m^2\,s^{-1}} \;\tilde{<}\; \kappa_t \;\tilde{<}\; 10^{-1}\ \mathrm{m^2\,s^{-1}} \quad . \tag{41}$$

The smallest values of the eddy coefficient are about 2 orders of magnitude larger than the highest values of the molecular diffusivity ($\approx 10^{-7}\ \mathrm{m^2\,s^{-1}}$). Therefore, the molecular fluxes are often disregarded, allowing us to transform (39) to the conservative form of the reactive transport equation that will be used hereinafter

$$\frac{\partial \overline{C}_n}{\partial t} \;=\; \overline{\theta}_n \;-\; \nabla\bullet(\overline{C}_n\overline{\mathbf{v}} - \kappa_t \nabla \overline{C}_n) \tag{42}$$

or, equivalently,

$$\frac{\partial \overline{C}_n}{\partial t} = \overline{\theta}_n - \frac{\partial}{\partial x}\left(\overline{C}_n \overline{u} - \kappa_t \frac{\partial \overline{C}_n}{\partial x} \right) - \frac{\partial}{\partial y}\left(\overline{C}_n \overline{v} - \kappa_t \frac{\partial \overline{C}_n}{\partial y} \right) - \frac{\partial}{\partial z}\left(\overline{C}_n \overline{w} - \kappa_t \frac{\partial \overline{C}_n}{\partial z} \right) \tag{43}$$

Taking into account the mean and fluctuating parts of the velocity, the Boussinesq version of the continuity equation (28) may be rewritten as follows: $\nabla \bullet (\overline{\mathbf{v}} + \tilde{\mathbf{v}}) = 0$. Applying the averaging operator to this equation leads to

$$\overline{\nabla \bullet (\overline{\mathbf{v}} + \tilde{\mathbf{v}})} = \nabla \bullet (\overline{\overline{\mathbf{v}} + \tilde{\mathbf{v}}}) = \nabla \bullet (\overline{\overline{\mathbf{v}}} + \overline{\tilde{\mathbf{v}}}) = \nabla \bullet \overline{\mathbf{v}} = 0 \tag{44}$$

Combining (42) and (44), we obtain the convective form of the reactive transport equation:

$$D_t \overline{C}_n = \left(\frac{\partial}{\partial t} + \overline{\mathbf{v}} \bullet \nabla \right) \overline{C}_n = \overline{\theta}_n + \nabla \bullet (\kappa_t \nabla \overline{C}_n) \tag{45}$$

or, equivalently,

$$\frac{\partial \overline{C}_n}{\partial t} + \overline{u} \frac{\partial \overline{C}_n}{\partial x} + \overline{v} \frac{\partial \overline{C}_n}{\partial y} + \overline{w} \frac{\partial \overline{C}_n}{\partial z} = \theta_n + \frac{\partial}{\partial x}\left(\kappa_t \frac{\partial \overline{C}_n}{\partial x} \right) + \frac{\partial}{\partial y}\left(\kappa_t \frac{\partial \overline{C}_n}{\partial y} \right) + \frac{\partial}{\partial z}\left(\kappa_t \frac{\partial \overline{C}_n}{\partial z} \right) \tag{46}$$

Taking the sum of (42) over all the constituents, we have

$$\frac{\partial}{\partial t} \underbrace{\sum_{n=0}^{N} \overline{C}_n}_{=1} = \underbrace{\sum_{n=0}^{N} \overline{\theta}_n}_{=0} - \nabla \bullet [\underbrace{\sum_{n=0}^{N} \overline{C}_n}_{=1} \overline{\mathbf{v}} - \kappa_t \nabla \underbrace{\sum_{n=0}^{N} \overline{C}_n}_{=1}] \tag{47}$$

which reduces to continuity equation (44), $\nabla \bullet \overline{\mathbf{v}} = 0$, as expected.

3.4. Boundary conditions for the reactive transport equation

Reactive transport equation (42) is of parabolic type. Accordingly, to solve it in domain Ω limited by boundary Γ (which is no longer assumed to be motionless), it is necessary to prescribe the initial value of the concentration in Ω and to impose one boundary condition on Γ. There exist various types of suitable boundary conditions for this equation: it must involve neither a time derivative nor space derivatives with an order higher than unity (e.g. Garabedian 1964). In addition, Γ may be split into several parts, on which the boundary conditions may be different.

For instance, the value of $\overline{C}_n$ may be imposed, possibly as a function of time and position, yielding a Dirichlet boundary condition. Conceptually, this type of boundary condition is simple, but is not always conducive to well-behaved solutions in numerical models, especially when imposed on an outgoing boundary ($\overline{\mathbf{v}} \bullet \mathbf{n} > 0$). Indeed, spurious oscillations of the concentrations may arise in the vicinity of such a boundary (e.g., Roache 1972).

Other boundary conditions involve the flux crossing the domain boundary. Integrating (42) over the domain, using the divergence and Reynolds' transport theorem (e.g., Deleersnijder 2019c), we obtain

$$\frac{d}{dt} \int_{\Omega} \overline{C}_n \, d\Omega = \int_{\Omega} \overline{\theta}_n \, d\Omega - \int_{\Gamma} [\overline{C}_n (\overline{\mathbf{v}} - \mathbf{v}^{\Gamma}) - \kappa_t \nabla \overline{C}_n] \bullet \mathbf{n} \, d\Gamma \tag{48}$$

where $\mathbf{v}^{\Gamma}$ denotes the velocity of the points of the domain boundary. Thus, the elemental

mass δm_n of the n-th constituent that leaves the domain during time interval $[t,t+\delta t]$ through surface element $\delta\Gamma$ tends to

$$\delta m_n \sim \rho_\bullet [\overline{C}_n(\overline{\mathbf{v}}-\mathbf{v}^\Gamma)-\kappa_t\nabla\overline{C}_n]\bullet\mathbf{n}\,\delta S\,\delta t \quad , \quad \delta t\to 0 \tag{49}$$

By the same token, the elemental mass of the mixture crossing the same surface element is

$$\begin{aligned}\delta m = \sum_{n=0}^{N}\delta m_n &\sim \rho_\bullet [\overbrace{\sum_{n=0}^{N}\overline{C}_n}^{=1}(\overline{\mathbf{v}}-\mathbf{v}^\Gamma)-\kappa_t\nabla\overbrace{\sum_{n=0}^{N}\overline{C}_n}^{=1}]\bullet\mathbf{n}\,\delta\Gamma\,\delta t \\ &\sim \rho_\bullet (\overline{\mathbf{v}}-\mathbf{v}^\Gamma)\bullet\mathbf{n}\,\delta\Gamma\,\delta t \quad , \quad \delta t\to 0\end{aligned} \tag{50}$$

If the outgoing mass flux $\rho_\bullet\Phi_n$ ($\mathrm{kg\,m^{-2}\,s^{-1}}$) is known, then the following Neumann boundary condition is to be prescribed:

$$\left[[\overline{C}_n(\overline{\mathbf{v}}-\mathbf{v}^\Gamma)-\kappa_t\nabla\overline{C}_n]\bullet\mathbf{n}\right]_{\mathbf{x}\in\Gamma} = \Phi_n \tag{51}$$

For gas exchanges at the air-water interface, Φ_n ($\mathrm{m\,s^{-1}}$) is usually evaluated by having recourse to the concept of piston velocity, yielding a Robin boundary condition in which the flux is of the form $\Phi_n=[\varpi(C-C^s)]_{\mathbf{x}\in\Gamma}$, where ϖ and C^s are the piston velocity and the relevant saturation concentration, respectively (e.g., Wanninkhof 1992, Jähne and Hauβecker 1998).

If the boundary is impermeable (no particle of any constituent crosses it), then the associated impermeability conditions read

$$\left[[\overline{C}_n(\overline{\mathbf{v}}-\mathbf{v}^\Gamma)-\kappa_t\nabla\overline{C}_n]\bullet\mathbf{n}\right]_{\mathbf{x}\in\Gamma} = 0 \quad , \quad n=0,1,\ldots N \tag{52}$$

For the whole fluid mixture, the impermeability condition is obtained directly from (50) or, equivalently, by taking the sum of (52) over all the constituents, yielding

$$\left[(\overline{\mathbf{v}}-\mathbf{v}^\Gamma)\bullet\mathbf{n}\right]_{\mathbf{x}\in\Gamma} = 0 \tag{53}$$

Combining (52) and (53) shows that, for each constituent, both the advective flux and the turbulent one are zero through an impermeable boundary:

$$\left.\begin{aligned}\left[[\overline{C}_n(\overline{\mathbf{v}}-\mathbf{v}^\Gamma)]\bullet\mathbf{n}\right]_{\mathbf{x}\in\Gamma} &= 0 \\ \left[(-\kappa_t\nabla\overline{C}_n)\bullet\mathbf{n}\right]_{\mathbf{x}\in\Gamma} &= 0\end{aligned}\right\} \quad n=0,1,\ldots N \tag{54}$$

If the impermeable boundary is motionless, then $\mathbf{v}^\Gamma=0$, which allows simplifying (54) to

$$\left.\begin{aligned}\left[\overline{C}_n\overline{\mathbf{v}}\bullet\mathbf{n}\right]_{\mathbf{x}\in\Gamma} &= 0 \\ \left[(-\kappa_t\nabla\overline{C}_n)\bullet\mathbf{n}\right]_{\mathbf{x}\in\Gamma} &= 0\end{aligned}\right\} \quad n=0,1,\ldots N \tag{55}$$

3.5. Turbulent momentum flux

In Section 3.3, the filtered macroscopic flux of a constituent, $\overline{C_n\mathbf{v}}$, has been split into two contributions, the resolved one, $\overline{C}_n\overline{\mathbf{v}}$, and the unresolved (turbulent) one, $\overline{\tilde{C}_n\tilde{\mathbf{v}}}$, which was parameterised à la Fourier-Fick, i.e. $\overline{\tilde{C}_n\tilde{\mathbf{v}}}=-\kappa_t\nabla\overline{C}_n$, by having recourse to the so-called turbulent (or eddy) diffusivity κ_t. Similarly, the turbulent macroscopic momentum flux (which is a second-order tensor) will be parameterised with the help of the so-called turbulent or eddy (kinematic) viscosity ν_t ($\mathrm{m^2\,s^{-1}}$).

Assuming that properties (35) hold valid for the velocity vector, the averaged momentum

flux reads:

$$\begin{aligned}\overline{\mathbf{v}\mathbf{v}} &= \overline{(\overline{\mathbf{v}}+\tilde{\mathbf{v}})(\overline{\mathbf{v}}+\tilde{\mathbf{v}})} = \overline{\overline{\mathbf{v}}\overline{\mathbf{v}}+\overline{\mathbf{v}}\tilde{\mathbf{v}}+\tilde{\mathbf{v}}\overline{\mathbf{v}}+\tilde{\mathbf{v}}\tilde{\mathbf{v}}} \\ &= \overline{\overline{\mathbf{v}}\overline{\mathbf{v}}} + \overline{\overline{\mathbf{v}}\underbrace{\tilde{\mathbf{v}}}_{=0}} + \overline{\underbrace{\tilde{\mathbf{v}}}_{=0}\overline{\mathbf{v}}} + \overline{\tilde{\mathbf{v}}\tilde{\mathbf{v}}} = \overline{\overline{\mathbf{v}}\overline{\mathbf{v}}} + \overline{\tilde{\mathbf{v}}\tilde{\mathbf{v}}}\end{aligned} \tag{56}$$

where the resolved flux is $\overline{\overline{\mathbf{v}}\overline{\mathbf{v}}}$, whilst $\overline{\tilde{\mathbf{v}}\tilde{\mathbf{v}}}$ is the unresolved (or turbulent) one and expression $-\rho_{\bullet}\overline{\tilde{\mathbf{v}}\tilde{\mathbf{v}}}$ is generally called the Reynolds stress tensor. It is tempting to have recourse to the following parameterisation: $\overline{\tilde{\mathbf{v}}\tilde{\mathbf{v}}} = -\nu_t \nabla\overline{\mathbf{v}}$. Though tensor $\overline{\tilde{\mathbf{v}}\tilde{\mathbf{v}}}$ is symmetric, parameterisation $-\nu_t \nabla\overline{\mathbf{v}}$ is not, rendering this expression unacceptable. This problem may be solved by turning to the modified parameterisation $\overline{\tilde{\mathbf{v}}\tilde{\mathbf{v}}} = -\nu_t\left[\nabla\overline{\mathbf{v}} + (\nabla\overline{\mathbf{v}})^T\right]$. This formula is not acceptable either, for the trace of the right-hand side is identically zero, $-2\nu_t\nabla\bullet\overline{\mathbf{v}} = 0$, whilst the trace of the left-hand side is not

$$\mathrm{tr}(\overline{\tilde{\mathbf{v}}\tilde{\mathbf{v}}}) = \overline{\tilde{\mathbf{v}}\bullet\tilde{\mathbf{v}}} = \overline{\tilde{u}\tilde{u}} + \overline{\tilde{v}\tilde{v}} + \overline{\tilde{w}\tilde{w}} = 2k \tag{57}$$

where the positive definite variable k is termed turbulence kinetic energy. Therefore, an acceptable parameterisation is

$$\begin{aligned}\overline{\tilde{\mathbf{v}}\tilde{\mathbf{v}}} &= -\nu_t\left[\nabla\overline{\mathbf{v}} + (\nabla\overline{\mathbf{v}})^T\right] + \frac{2}{3}k\mathbf{I} \\ &= \begin{pmatrix} -\nu_t\left(\frac{\partial\overline{u}}{\partial x}+\frac{\partial\overline{u}}{\partial x}\right)+\frac{2}{3}k & -\nu_t\left(\frac{\partial\overline{u}}{\partial y}+\frac{v\partial\overline{v}}{\partial x}\right) & -\nu_t\left(\frac{\partial\overline{u}}{\partial z}+\frac{\partial\overline{w}}{\partial x}\right) \\ -\nu_t\left(\frac{\partial\overline{v}}{\partial x}+\frac{\partial\overline{u}}{\partial y}\right) & -\nu_t\left(\frac{\partial\overline{v}}{\partial y}+\frac{\partial\overline{v}}{\partial y}\right)+\frac{2}{3}k & -\nu_t\left(\frac{\partial\overline{v}}{\partial z}+\frac{\partial\overline{w}}{\partial y}\right) \\ -\nu_t\left(\frac{\partial\overline{w}}{\partial x}+\frac{\partial\overline{u}}{\partial z}\right) & -\nu_t\left(\frac{\partial\overline{w}}{\partial y}+\frac{\partial\overline{v}}{\partial z}\right) & -\nu_t\left(\frac{\partial\overline{w}}{\partial z}+\frac{\partial\overline{w}}{\partial z}\right)+\frac{2}{3}k \end{pmatrix}\end{aligned} \tag{58}$$

where $\mathbf{I}$ is the identity tensor, i.e. $\mathbf{I} = diag(1,1,1)$. It is also important to note that $\nabla\overline{\mathbf{v}}$ is not invariant under a rotation of the coordinate system whereas $\nabla\overline{\mathbf{v}} + (\nabla\overline{\mathbf{v}})^T$ and $\mathbf{I}$ are (e.g. Chavez 2013).

In estuarine and marine flows, the eddy viscosity may exhibit a wide range of variation:

$$10^{-5}\,\mathrm{m^2\,s^{-1}} \lesssim \nu_t \lesssim 10^{-1}\,\mathrm{m^2\,s^{-1}} \tag{59}$$

At any time and position, the turbulent diffusivity and viscosity are different, but are always of the same order of magnitude. The smallest values of the kinematic turbulent viscosity are about one of magnitude larger than the highest values of the molecular diffusivity ($\approx 10^{-6}\ \mathrm{m^2\,s^{-1}}$). Therefore, the molecular momentum fluxes are often disregarded.

4. Properties of the solution of the reactive transport equation

From here on and until otherwise stated, only averaged variables will be dealt with. Therefore, for notational simplicity, the overbars will be systematically omitted. Similarly, when the concentration of only one constituent will be considered, the subscript identifying this constituent will be omitted.

To help comprehend the markedly different roles of advection and diffusion, it is instructive to study transport problems of which the analytical solution exist or properties of the solution can be established analytically. In this respect, we will first solve a classical one-

dimensional advection-diffusion equation.

4.1. One-dimensional advection-diffusion problem

Consider the evolution of the concentration $C(t,x)$ of a passive tracer in the infinite domain $x \in]-\infty,\infty[$. Let the positive constants U and K represent velocity and diffusivity. The concentration obeys the equation

$$\frac{\partial C}{\partial t} + U\frac{\partial C}{\partial x} = K\frac{\partial^2 C}{\partial x^2} \tag{60}$$

The initial tracer distribution is assumed to be a "Morse dash":

$$C(0,x) = \begin{cases} C^0, & x \in]-L,L[\\ 0, & x \notin]-L,L[\end{cases} \tag{61}$$

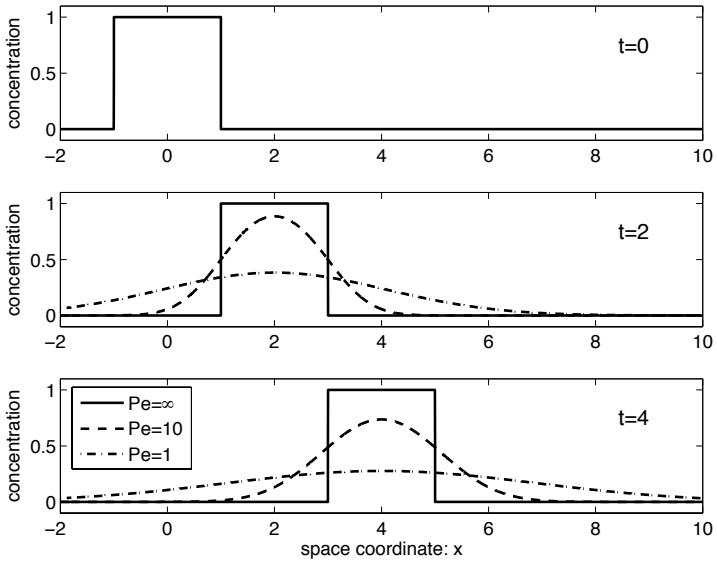


Figure 4. Representation of concentration (68) at different instants for various values of the Peclet number. The smaller the value of the latter, the stronger the impact of diffusion. In the limit $Pe \to \infty$, diffusion is negligible and advection is the only significant transport phenomenon. Irrespective of the value of the Peclet number, the point where the concentration is maximum moves at the same speed, which is equal to unity since dimensionless variables (65) are used.

Irrespective of the initial tracer distribution, diffusion and advection proceed independently. The latter causes a drift at velocity U in the direction of increasing x that does not impact diffusion. This may be seen by having recourse to a Galilean transformation. The new variables are: $t^* = t$ and $x^* = x - Ut$; the origin of the new space coordinate moves at speed U in the direction of increasing x. Then, the differential operators transform to

$$\frac{\partial}{\partial t} = \underbrace{\frac{\partial t^*}{\partial t}}_{=1}\frac{\partial}{\partial t^*} + \underbrace{\frac{\partial x^*}{\partial t}}_{=-U}\frac{\partial}{\partial x^*} = \frac{\partial}{\partial t^*} - U\frac{\partial}{\partial x^*} \tag{62}$$

$$\frac{\partial}{\partial x} = \underbrace{\frac{\partial t^*}{\partial x}}_{=0}\frac{\partial}{\partial t^*} + \underbrace{\frac{\partial x^*}{\partial x}}_{=1}\frac{\partial}{\partial x^*} = \frac{\partial}{\partial x^*} \tag{63}$$

Substituting (62)-(63) into (60) leads to the diffusion equation

$$\frac{\partial C}{\partial t^*} = K\frac{\partial^2 C}{\partial x^{*2}} \tag{64}$$

This shows that, as stated above, diffusion is not impacted by the drift at velocity U, which affects all of the tracer particles in the same manner at any time and position.

It is convenient to introduce dimensionless variables:

$$t' = \frac{t}{L/U}\ , \quad x' = \frac{x}{L}\ , \quad C' = \frac{C}{C^0} \tag{65}$$

In this subsection, from here on, only dimensionless variables will be used. Thus, to simplify notations, the primes will be systematically omitted. Hence, the equation and the initial condition are

$$\frac{\partial C}{\partial t} + \frac{\partial C}{\partial x} = \frac{1}{Pe}\frac{\partial^2 C}{\partial x^2} \tag{66}$$

$$C(0,x) = \begin{cases} 1, & x \in]-1,1[\\ 0, & x \notin]-1,1[\end{cases} \tag{67}$$

where $Pe = UL/K$ denotes the Peclet number, which represents the ratio of the order of magnitude of the advection term to the diffusion one — under the assumption that L is a suitable length scale, which is disputable since the domain of interest is unbounded. The exact solution of (66)-(67) is

$$C(t,x) = \frac{1}{2}\,\mathrm{erf}\left(\frac{1+t-x}{\sqrt{4t/Pe}}\right) - \frac{1}{2}\,\mathrm{erf}\left(\frac{-1+t-x}{\sqrt{4t/Pe}}\right) \tag{68}$$

where "erf" denotes the error function[4]. Figure 4 illustrates the impact of the Peclet number on expression (68).

The one-dimensional example above is somewhat misleading in that it might lead one to believe that the effect of advection and that of diffusion can always be clearly separated. This holds valid in a one-dimensional flow, but not in multi-dimensional ones. For instance, Figure 2 of Welander (1955) vividly illustrates the deformation of a chessboard pattern by pure two-dimensional advection in the atmosphere. This reversible phenomenon, often referred to as stirring, creates small-scale structures, which may ultimately enhance the impact of diffusion, which is irreversible — but is absent in this case.

4.2. Mass conservation and concentration homogenisation

The mass budget of various constituents over the domain of interest is often to be taken into consideration. The simplest version of the related manipulations is presented below.

Let the time-independent volume and surface Ω and Γ represent the domain of interest and the boundary delimiting it, respectively. The volume of the domain is

[4] See, e.g., https://mathworld.wolfram.com/Erf.html (last viewed on 22 August 2023)

$$V = \int_{\Omega} d\Omega \tag{69}$$

Domain Ω is assumed to isolated from its environment, implying that there is no net flux of the fluid mixture crossing its boundary:

$$\left[\mathbf{v}\bullet\mathbf{n}\right]_{\mathbf{x}\in\Gamma} = 0 \tag{70}$$

Concentration $C(t,\mathbf{x})$ of a passive tracer present in the domain of interest obeys the equation

$$\frac{\partial C}{\partial t} = -\nabla\bullet(C\mathbf{v}-\kappa_t\nabla C) \tag{71}$$

The eddy diffusivity is positive, but is not necessarily a constant, i.e., $\kappa_t(t,\mathbf{x})>0$. The initial concentration distribution, $C(0,\mathbf{x}) = C^0(\mathbf{x})$, is a known, non-negative function of the position. Since the domain boundary is impermeable, the following boundary condition is to be enforced:

$$[(-\kappa_t\nabla C)\bullet\mathbf{n}]_{\mathbf{x}\in\Gamma} = 0 \tag{72}$$

Now integrate over the domain of interest the left-hand side of (71):

$$\int_{\Omega}\frac{\partial C}{\partial t}\,d\Omega = \frac{\partial}{\partial t}\underbrace{\int_{\Omega} C\,d\Omega}_{\substack{=m(t)/\rho_\bullet \\ \text{see (30)}}} = \frac{1}{\rho_\bullet}\frac{dm}{dt} \tag{73}$$

where $m(t)$ is the mass of the tracer present in the domain at time t. Then, integrating over Ω the right-hand side of (71), using the divergence theorem and boundary conditions (70) and (72) yields

$$\int_{\Omega}\nabla\bullet(C\mathbf{v}-\kappa_t\nabla C)\,d\Omega = \int_{\Gamma}\underbrace{(C\mathbf{v}-\kappa_t\nabla C)\bullet\mathbf{n}}_{=0,\ \text{see (70) and (72)}}\,d\Gamma = 0 \tag{74}$$

Next, combining (73) and (74) leads to $dm/dt = 0$ and, hence, $m(t) = m(0)$. Thus, the mass of tracer is conserved. This result is far from unexpected. Since the tracer is passive, it is neither produced nor destroyed inside the domain. The latter is isolated from its environment, implying that no tracer particle crosses the boundary. It must be underscored that this result has been obtained without any prior knowledge of the exact solution of the partial differential problem governing the evolution of concentration $C(t,\mathbf{x})$.

If we assume for a moment that the tracer undergoes a first-order decay process characterised by constant mean life τ, then the corresponding concentration and mass would simply be $e^{-t/\tau}C(t,\mathbf{x})$ and $e^{-t/\tau}m(t)$. This is because there is no flux through the domain boundary and the decay process takes place at the same rate at any time and location.

The domain-averaged concentration of the passive tracer is $\overline{C} = m(0)/(\rho_\bullet V)$. Then, introduce $\hat{C}(t,\mathbf{x}) = C(t,\mathbf{x}) - \overline{C}$, i.e. the deviation of the concentration with respect to its domain-averaged value. The integral over the domain of $\hat{C}(t,\mathbf{x})$ is readily seen to be identically zero at any time.

The concentration deviation satisfies advection-diffusion equation

$$\frac{\partial \hat{C}}{\partial t} = -\nabla\bullet(\hat{C}\mathbf{v}-\kappa_t\nabla\hat{C}) \tag{75}$$

under boundary condition $[(-\kappa_t \nabla \hat{C}) \bullet \mathbf{n}]_{\mathbf{x} \in \Gamma} = 0$. Then, we multiply (75) by $\hat{C}$ and, after some manipulations, we obtain relation

$$\frac{\partial \hat{C}^2}{\partial t} = -\nabla \bullet (\hat{C}^2 \mathbf{v}) + 2\nabla \bullet (\hat{C} \kappa_t \nabla \hat{C}) - 2\kappa_t \left| \nabla \hat{C} \right|^2 \tag{76}$$

which we integrate over the domain of interest. Taking into account the impermeability boundary conditions leads to

$$\frac{d\sigma^2}{dt} = -\frac{2}{V} \int_{\Omega} \kappa_t \left| \nabla \hat{C} \right|^2 d\Omega < 0 \tag{77}$$

where

$$\sigma^2(t) = \frac{1}{V} \int_{\Omega} [\hat{C}(t,\mathbf{x})]^2 \, d\Omega \tag{78}$$

is the variance of the concentration, i.e., a positive-definite global measure of the heterogeneity of the concentration.

As $\kappa_t > 0$ at any time and location, the variance of the concentration will decrease monotonously. In other words, as time progresses the tracer concentration will progressively homogenise until a constant, uniform value is arrived at, i.e.,

$$\lim_{t \to \infty} \hat{C}(t,\mathbf{x}) = 0 \tag{79}$$

or, equivalently,

$$\lim_{t \to \infty} C(t,\mathbf{x}) = \overline{C} \tag{80}$$

Clearly, it is (turbulent) diffusion that causes the concentration contrasts to decrease. Advection has no direct impact thereon, but is likely to influence the rate of homogenisation. It must be stressed that the results obtained in this subsection did not require any knowledge of the exact solution of the tracer transport problem under consideration. They are applicable to any passive tracer transported by advection and diffusion in a domain isolated from its environment, irrespective of its shape. These properties are thus rather general. It is noteworthy that similar results may be derived if the fluid mixture is compressible (e.g. Deleersnijder 2012).

4.3. Behaviour of concentration extrema

We will revisit the problem of the previous subsection in order to gain insight into the behaviour of concentration extrema. Assume that a local maximum of the concentration is located at a point whose position vector is denoted $\mathbf{r}(t)$. Then, the concentration must satisfy the following properties: $[\nabla C]_{\mathbf{x}=\mathbf{r}(t)} = 0$ and $[\partial^2 C / \partial \xi^2]_{\mathbf{x}=\mathbf{r}(t)} \leq 0$, with $\xi = x,y,z$. The time rate of change of the concentration at $\mathbf{x} = \mathbf{r}(t)$ is

$$\frac{d}{dt} C[t,\mathbf{r}(t)] = \left[\frac{\partial C}{\partial t} + \frac{d\mathbf{r}}{dt} \bullet \nabla C \right]_{\mathbf{x}=\mathbf{r}(t)} \tag{81}$$

Then, transforming (71) to

$$\frac{\partial C}{\partial t} = (-\mathbf{v} + \nabla \kappa_t) \bullet \nabla C + \kappa_t \nabla^2 C \tag{82}$$

and combining this relation with (81), we obtain

$$\frac{d}{dt}C[t,\mathbf{r}(t)] = \underbrace{\left[\left(-\mathbf{v}+\frac{d\mathbf{r}}{dt}+\nabla\kappa_t\right)\bullet\nabla C\right]_{\mathbf{x}=\mathbf{r}(t)}}_{=0} + \underbrace{\left[\kappa_t\nabla^2 C\right]_{\mathbf{x}=\mathbf{r}(t)}}_{\leq 0} \leq 0 \qquad (83)$$

Therefore, as a result of the action of diffusion, the local maximum value of the concentration cannot increase. This does not imply, however, that the position of the concentration maximum is motionless. A similar reasoning may be resorted to demonstrate that, as a result of the action of diffusion, a local minimum value of the concentration cannot decrease.

That a local concentration maximum (resp. minimum) cannot increase (resp. decrease) is in agreement with diffusive processes causing the tracer concentration field to progressively homogenise.

The method introduced in this subsection does not allow us to take into account the impact of the boundary conditions, nor does it allow for the impact of reactive processes to be easily taken into account. To do so, a global method must be resorted to. Specifically, to demonstrate that $C(t,\mathbf{x}) \geq C_{\min}(t)$[5], we have to show that the L^2-norm of the negative part of $C - C_{\min}$, which is defined as $\left[(C-C_{\min})-\left|C-C_{\min}\right|\right]/2$, remains zero. Similarly, showing that the L^2-norm of the positive part of $C - C_{\max}$, i.e. $\left[(C-C_{\max})+\left|C-C_{\max}\right|\right]/2$, remains zero implies that $C(t,\mathbf{x}) \leq C_{\max}(t)$. The necessary mathematical developments are not straightforward, since the positive part or the negative part of a function is not differentiable on the surface where this function is zero as is pointed out in Appendix C of Deleersnijder et al. (2001). Since this approach relies on the study of the L^2-norm of the relevant functions, it is often referred to as an energy method. This allows local properties to be established for any domain of interest and for a wide class of boundary conditions without requiring the prior determination of the exact solution of the problem under consideration. Clearly, the energy method is powerful and versatile. It can be applied to a large number of partial differential problems (e.g., Lewandowski 1997, Legrand et al. 2006, Blaise and Deleersnijder 2008, de Brye et al. 2012, Deleersnijder 2019d).

4.4. First-order decay and diffusion in a simple water column model

Studying the penetration into the sea of substances originating from the atmosphere, be they naturally occurring or human-made, is ripe with lessons to be learned about reactive transport processes. Presumably, the simplest model that can be conceived is a "water column model"[6]. The latter is based on several assumptions, the most important of which is horizontal homogeneity. Accordingly, if t and z denote the time and a vertical coordinate (with $z=-h$ at the ocean bottom and $z=0$ at the water-air interface), the concentration $C(t,z)$ of a constituent (or tracer) dissolved in the water that undergoes a first-order decay process and is originating from the atmosphere obeys

[5] $C_{\min}(t) = \min_{\mathbf{x}\in\Omega} C(t,\mathbf{x})$, $C_{\max}(t) = \max_{\mathbf{x}\in\Omega} C(t,\mathbf{x})$

[6] See, e.g., https://gotm.net/portfolio/ (last viewed on 28 August 2023)

$$\begin{cases} \dfrac{\partial C}{\partial t} = -\lambda C + K\dfrac{\partial^2 C}{\partial z^2} \\ C(0,z) = 0\,, \quad C(t,0) = C^s\,, \quad \left[-K\dfrac{\partial C}{\partial z}\right]_{z=-h} = 0 \end{cases} \tag{84}$$

where positive constants λ, K and C^s denote the rate of decay of the tracer under consideration (its mean life is $1/\lambda$), the vertical diffusivity and the prescribed surface concentration, respectively.

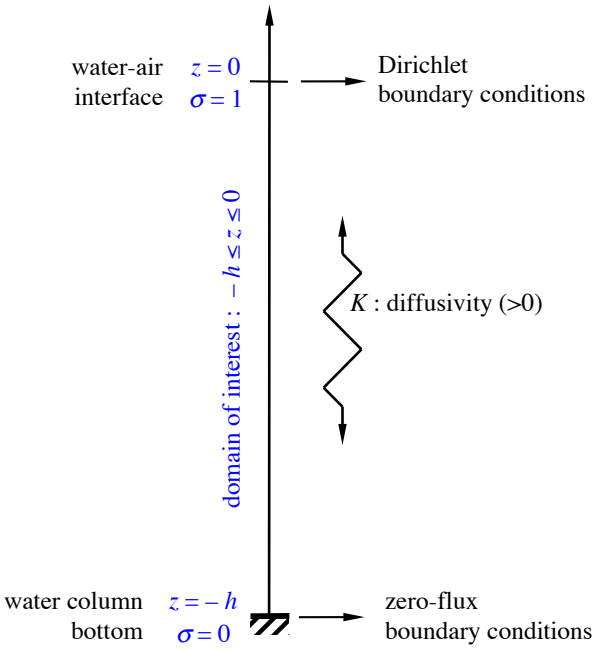


Figure 5. Illustration of the geometry and boundary conditions of the water column model under consideration in Section 4.4. The lower boundary (i.e., the seabed) is impermeable, whilst the sea surface is permeable. The tracer flux through it is always directed from the atmosphere toward the water column.

In light of (84), there is no flux through the lower boundary of the domain (i.e., the seabed), which is thus impermeable. The upper boundary (i.e., the water-air interface) is permeable. The concentration is always maximum on this boundary. Thus, the vertical derivative of the concentration at the sea surface is always non-negative, $\left[\partial C/\partial z\right]_{z=0} \ge 0$, implying that the tracer flux through the upper domain boundary is always directed from the atmosphere towards the sea.

Multiplying the governing equations by reference density ρ_*, integrating them over a water column with constant cross-sectional area S and taking into account the boundary conditions leads to

$$\frac{d}{dt}\underbrace{\int_{-h}^{0}\rho_{\bullet}SC\,dz}_{=m(t)} = -\lambda\underbrace{\int_{-h}^{0}\rho_{\bullet}SC\,dz}_{=m(t)} + \underbrace{\left[\rho_{\bullet}SK\frac{\partial C}{\partial z}\right]_{z=0}}_{=\Phi^{s}(t)} - \underbrace{\left[\rho_{\bullet}SK\frac{\partial C}{\partial z}\right]_{z=-h}}_{=0,\ \text{see (84)}} \tag{85}$$

where $m(t)$ and $\Phi^{s}(t)$ (≥ 0) denote the mass of tracer present in the domain and the tracer flux (kg/s) that crosses the upper boundary, respectively. Since, the initial concentration is zero, the tracer mass is the solution of

$$\begin{cases}\dfrac{dm}{dt} = -\lambda m + \Phi^{s} \\ \left[m(t)\right]_{t=0} = 0\end{cases} \tag{86}$$

eventually yielding

$$m(t) = \int_{0}^{t}\Phi^{s}(t-t')e^{-\lambda t'}\,dt' \tag{87}$$

In the present model, the mass of tracer contained in the water column under considered cannot decrease. To explicitly calculate convolution product (87), we need to determine the surface flux, which can be achieved by solving (84).

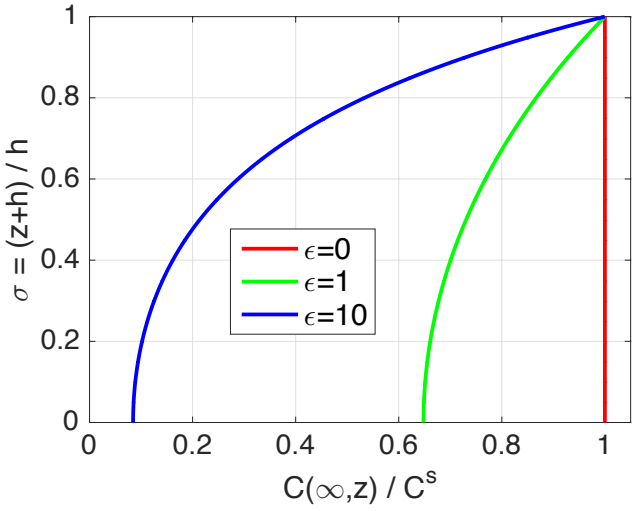


Figure 6. Steady-state profile of the concentration for various values of the Damköhler number ($\varepsilon = 0, 1, 10$). The concentrations at the top of the water column are equal to each other. The vertical derivative of the concentrations is zero at the ocean bottom (impermeability condition).

The solution of differential problem (84) reads

$$\frac{C(t,z)}{C^{s}} = \frac{\cosh(\sigma\sqrt{\varepsilon})}{\cosh(\sqrt{\varepsilon})} + \sum_{n=0}^{\infty} c_n \exp\left[-(\varepsilon + k_n^2)\tau\right]\cos(k_n\sigma) \tag{88}$$

with $\sigma = (z+h)/h$, $k_n = (n+1/2)\pi$, $c_n = 2(-1)^{n+1}k_n/(\varepsilon + k_n^2)$, and

$$\tau = \frac{t}{h^2/K} = \frac{\text{time}}{\text{diffusion timescale}} \tag{89}$$

$$\varepsilon = \frac{\lambda h^2}{K} = \frac{h^2/K}{1/\lambda} = \frac{\text{diffusion timescale}}{\text{decay timescale}} \tag{90}$$

where dimensionless parameter ε is often referred to as the "Damköhler number".

The concentration tends to a steady-state profile (Figure 6), i.e.,

$$C(\infty,z) = \lim_{t\to\infty} C(t,z) = \frac{\cosh(\sigma\sqrt{\varepsilon})}{\cosh(\sqrt{\varepsilon})} C^s \tag{91}$$

Clearly, (88) consists of a steady-state part, which is the first term in its right-hand side, i.e., $C(\infty,z)$, and a sum of an infinite number of modes decreasing exponentially as time progresses. It is readily seen that larger the order of the mode (i.e., n), the faster the decay. As a consequence, the typical time for the concentration to approach the steady-state limit is related to the mode exhibiting the slowest rate of decay, i.e., the $n=0$ mode. For the latter, the exponential term may be transformed as follows:

$$\exp\left[-(\varepsilon + k_0^2)\tau\right] = \exp\left(-\frac{t}{T}\right) \tag{92}$$

where T denotes the adjustment timescale,

$$T = \frac{h^2/K}{\varepsilon + \pi^2/4} \tag{93}$$

If the decay process is much slower than vertical mixing, then the Damköhler number is small. In this case, adjustment timescale (93) admits asymptotic expression

$$T \sim \frac{4h^2}{\pi^2 K} - \frac{16h^2}{\pi^4 K}\varepsilon \ , \quad \varepsilon \to 0 \tag{94}$$

If, on the other hand, decay is much faster than vertical mixing, we obtain

$$T \sim \frac{h^2}{K\varepsilon} \sim \frac{1}{\lambda} \ , \quad \varepsilon \to \infty \tag{95}$$

Unsurprisingly, the steady-state concentration is constant if the decay rate is zero (passive tracer), i.e., $C(\infty,z) = C^s$. If the constituent actually decays ($\varepsilon > 0$), then the concentration is independent of the decay rate at the ocean surface, $C(\infty,0) = C^s$, and is easily seen to be a decreasing function of the decay rate at the ocean bottom, i.e.,

$$\frac{\partial}{\partial\varepsilon}\left[\frac{C(\infty,-h)}{C^s}\right] = -\frac{\sinh(\sqrt{\varepsilon})}{2\sqrt{\varepsilon}\cosh^2(\sqrt{\varepsilon})} < 0 \tag{96}$$

In fact, in accordance with elementary physical intuition, the concentration is a decreasing function of the decay rate at any location below the surface ($\sigma < 1$):

$$\frac{\partial}{\partial\varepsilon}\left[\frac{C(\infty,z)}{C^s}\right] = -\frac{\sinh[(1-\sigma)\sqrt{\varepsilon}] + (1-\sigma)\sinh(\sigma\sqrt{\varepsilon})\cosh(\sqrt{\varepsilon})}{2\sqrt{\varepsilon}\cosh^2(\sqrt{\varepsilon})} < 0 \tag{97}$$

Figure 6 illustrates this discussion.

There exist many other analytical solutions (e.g., Fischer et al. 1979, Rutherford 1994, Deleersnijder 2007, 2011), which may be instrumental in the validation of numerical models.

5. Numerical simulation

5.1. Small aspect ratio flows

As we mentioned briefly in Section 1, most of the flows of interest are likely to be viewed as "shallow", which refers to flows characterised by a small aspect ratio (δ) (Table 1). This (dimensionless) parameter is defined as the ratio of the vertical length scale, L_v, to the horizontal one, L_h, i.e., $\delta = L_v / L_h$. We must take into account the smallness of the aspect ratio when scaling the governing equations (i.e., estimating the relative order of magnitude of their terms). More precisely, the equations are to be scaled in a different manner in the vertical direction and on the horizontal plane. Accordingly, the del operator must be expressed as follows: $\nabla = \nabla_h + \mathbf{e}_z \partial / \partial z$, where ∇_h is the horizontal part of ∇, whilst $\mathbf{e}_z$ and z denote a vertical unit vector and the related vertical coordinate, respectively. By the same token, the horizontal velocity ($\mathbf{u}$) must be distinguished from the vertical one ($w\mathbf{e}_z$), yielding $\mathbf{v} = \mathbf{u} + w\mathbf{e}_z$. Then, the Boussinesq version of continuity equation (28) transforms to

$$\nabla \bullet \mathbf{v} = \nabla_h \bullet \mathbf{u} + \frac{\partial w}{\partial z} = 0 \tag{98}$$

Let U and W represent the horizontal velocity scale and the typical vertical velocity, then (98) implies

$$\frac{U}{L_h} \approx \frac{W}{L_v} \quad \Rightarrow \quad W \approx \frac{L_v}{L_h} U \approx \delta U << U \tag{99}$$

Since $\delta << 1$, the vertical velocity is generally much smaller than the horizontal one, but may be relatively noisy in hydrostatic models[7] (e.g., Deleersnijder and Wolanski 1990).

Table 1. Typical orders of magnitude of the horizontal length scale (L_h) and the vertical one (L_v), and the associated aspect ratio (δ) for an estuary (e.g., the Scheldt Estuary), a shelf sea (e.g., the North Sea) and a (deep) ocean (e.g., the Atlantic).

domain	L_h	L_v	$\delta = L_v / L_h$
estuary	$\approx 10^4$ m	≈ 10 m	$\approx 10^{-3}$
shelf sea	$\approx 10^5$ m	$\approx 10^2$ m	$\approx 10^{-3}$
(deep) ocean	$\approx 10^6$ m	$\approx 10^3$ m	$\approx 10^{-3}$

In light of the above considerations, reactive transport equation (42) should be rewritten as follows:

[7] In models relying on the hydrostatic equilibrium, the vertical velocity is obtained by integrating over the vertical direction continuity equation (84). In non-hydrostatic models, the calculation method of the vertical velocity is completely different (e.g., Marshall et al. 1997).

$$\frac{\partial C_n}{\partial t} = \theta_n - \nabla_h \bullet (C_n \mathbf{u} - \kappa_t \nabla_h C_n) - \frac{\partial}{\partial z}\left(C_n w - \kappa_t \frac{\partial C_n}{\partial z} \right) \tag{100}$$

Despite the vertical velocity being much smaller than the horizontal one, the advective terms in (46) are of the same order of magnitude:

$$\frac{\left| \nabla_h \bullet (C_n \mathbf{u}) \right|}{\left| \frac{\partial}{\partial z}(C_n w) \right|} \approx \underbrace{\frac{U / L_h}{W / L_v}}_{\text{see (99)}} \approx 1 \tag{101}$$

On the other hand, the order of magnitude of the diffusive terms are such that

$$\frac{\left| \nabla_h \bullet (\kappa_t \nabla_h C_n) \right|}{\left| \frac{\partial}{\partial z}\left(\kappa_t \frac{\partial C_n}{\partial z} \right) \right|} \approx \frac{1 / L_h^2}{1 / L_v^2} \approx \left(\frac{L_v}{L_h} \right)^2 \approx \underbrace{\delta^2 << 1}_{\text{see Table 1}} \tag{102}$$

As a result, (100) simplifies to

$$\frac{\partial C_n}{\partial t} = \theta_n - \nabla_h \bullet (C_n \mathbf{u}) - \frac{\partial}{\partial z}\left(C_n w - \kappa_t \frac{\partial C_n}{\partial z} \right) \tag{103}$$

Although we did not state it explicitly above, turbulent diffusivity κ_t is meant to help parameterise the impact of unresolved motions whose aspect ratio is of order unity, i.e., micro-turbulence, boundary layer turbulence, turbulence induced by the breaking of short internal waves, etc. There are, however, phenomena characterised by a small aspect ratio that cannot be resolved in the present approach. We can take them into account by introducing into (103) another term relying on a diffusivity, denoted κ_h, that is much larger than κ_t. Since this diffusivity is related to essentially horizontal phenomena (hence the subscript "*h*"), the simplest form of the associated "turbulent flux" reads $-\kappa_h \nabla_h C_n$, so that (103) transforms to

$$\frac{\partial C_n}{\partial t} = \theta_n - \nabla_h \bullet (C_n \mathbf{u} - \kappa_h \nabla_h C_n) - \frac{\partial}{\partial z}\left(C_n w - \kappa_t \frac{\partial C_n}{\partial z} \right) \tag{104}$$

In more than one case, diffusivity κ_h is assumed to be constant, whose value is to be calibrated. We can also have recourse to Smagorinsky (1963) (e.g., Shapiro et al. 2013) or Okubo (1971, 1976) (e.g., Duquesne et al. 2021, Vaz et al. 2022).

5.2. Numerical schemes for advection, diffusion and reactions

In most, if not all models, the horizontal diffusivity terms is smaller than all the other terms of (104), but it cannot be disregarded as it also likely to help ensure the stability of the numerical scheme used to discretise (104) and "damp small-scale computational noise" (Blumberg and Mellor 1987). We must also realise that it may be deemed to be appropriate to opt for a formulation of the "horizontal diffusion" term depending on the vertical coordinate system on which the discretisation is based (e.g., Mellor and Blumberg 1985). As a consequence, the general formulation of reactive transport equation (104) is

$$\frac{\partial C_n}{\partial t} = \theta_n - \nabla \bullet (C_n \mathbf{v} - \mathbf{K} \bullet \nabla C_n) \tag{105}$$

where $\mathbf{K}$ is the relevant diffusivity tensor, the simplest form of which is $\mathbf{K} = \mathrm{diag}(\kappa_h, \kappa_h, \kappa_t)$. In this case, (104) and (105) are equivalent to each other. Diffusivity tensor must be

symmetric and positive definite (e.g., Deleersnijder 2012). If we rely on (105) rather than (42), (77) transforms to

$$\frac{d\sigma^2}{dt} = -\frac{2}{V}\int_{\Omega} \nabla\hat{C} \bullet \mathbf{K} \bullet \nabla\hat{C}\, d\Omega < 0 \tag{106}$$

The properties established in Sections 4.2 and 4.3 remain valid (e.g., Deleersnijder 2012).

Mass budget (48) may help in the construction of discrete methods for obtaining an approximate solution of the reactive transport equation, especially conservative finite difference or finite volume schemes, be they based on a fixed mesh or a moving one. In the latter case, one may have recourse to the arbitrary Lagrangian-Eulerian approach (Hirt et al. 1974) or a discretisation technique directly or indirectly derived from it (e.g., Gerdes 1993, Delandmeter et al. 2018).

Numerical solutions are always imperfect. They must be assessed in order to determine to what extent they are capable of addressing the issues at hand, i.e. relevant validation activities must be performed (e.g., Willmott 1981, Oreskes et al. 1994, Dee 1995, Lynch and Davies 1995, Taylor 2001, Warner et al. 2005, Vallaeys et al. 2018). To do so, the results established in Sections 4.1-4 are likely to be of use. For instance, it may be necessary to guarantee that there is no spurious production or destruction of the constituent under consideration, in which case the scheme is termed conservative (e.g. White et al. 2008). The behaviour of extrema in the advection scheme must also be examined in detail (Thuburn 1997). If the diffusivity tensor is not diagonal, the discretisation of the corresponding term is unlikely to be straightforward (e.g., Beckers et al. 1998). Discrete reactive terms should be such that the numerical solution is positive, conservative and sufficiently accurate (Burchard et al. 2003, Kopecz and Meister 2019). Obviously, building, assessing and using simulation tools for estuaries and shelf seas is a multi-faceted endeavour, requiring the collaboration of researchers and practitioners from a wide range of disciplines (Fringer et al. 2019).

All of the above considerations are of a Eulerian nature, i.e., the concentrations are treated as functions of time and space. Needless to say, advection and diffusion can de tackled in a Lagrangian manner. See, for instance, van Sebille et al. (2018) and the references in this review article. It is noteworthy that a poorly-documented shortcoming of Lagrangian methods lies in the fact that a large number of particles must be seeded into the domain of interest to obtain accurate concentration fields, possibly requiring greater computational resources than their Eulerian counterparts to achieve the same level of accuracy. What is worse, estimating a priori the minimum number of particles needed is not as straightforward as one would like. Useful guidelines, however, exist (Silverman 1986, Spivakovskaya et al. 2007a). In addition, if the diffusivity tensor exhibits large space variations (e.g., in the vicinity of a sharp pycnocline), then it may be necessary to have recourse to rather elaborate Lagrangian methods (e.g., Stijnen et al. 2006, Spivakovskaya et al. 2007b, Gräwe et al. 2012).

We should bear mind that "well designed Eulerian and Lagrangian schemes converge to the exact solution as the space and time increments decrease for the former methods, and as the time resolution and the number of particles are increased for the latter. Therefore, discrepancies between Eulerian and Lagrangian simulation results are always due to numerical inaccuracies (or an erroneous implementation) and, hence, must not be ascribed to supposedly irreconcilable differences between the two approaches" (adapted from

Deleersnijder 2020a).

5.3. Ecological modelling

Reactive transport equations were solved numerically to serve countless purposes. One of them is ecological modelling. Equations of various levels of complexity were dealt with in three dimensions (e.g., Moll and Radach 2003, Radtke et al. 2012, Mouchet 2013, Groβe et al. 2019, Duquesne et al. 2021), and in two dimensions in a depth-integrated approach (e.g., Schuchert et al. 2018, Gross et al. 2023), a reduced-gravity one (e.g., Naithani et al. 2011) or a "horizontal-vertical" model (e.g., Lucas et al. 2009a). One-dimensional section-integrated (e.g., Naithani et al. 2016) or (vertical) water column (e.g., Lacroix and Nival 1998, Raick et al. 2007). Box or compartmental models were also used, with one box (e.g., Fasham et al. 1990, Davenport et al. 2012, Heinle and Slawig 2013), two boxes (e.g., Mata Almonacid and Medel 2022) or more (e.g., Raillard and Ménesguen 1994). It must be underscored that the fluxes between boxes were sometimes estimated in a rather casual manner, thereby ignoring some of the theoretical underpinning of such models (e.g., Lasaga 1980, Deleersnijder 2014).

6. Additional remarks

Sediment particles must be taken into account in many studies, because they may be of interest on their own (e.g., Gourgue et al. 2013, Wang et al. 2022) or pollutants are adsorbed on them (e.g., de Brauwere et al. 2014, Elskens et al. 2014). Traditionally (and, perhaps, somewhat unfortunately), sediment particles are not dealt with in the averages developed in Section 2.1. As a result, their (vertical) settling velocity, w^s (≥ 0), has to be included explicitly in the relevant transport equation, which usually reads (e.g., Xiong and Shen 2022)

$$\frac{\partial C_n}{\partial t} = -\nabla\bullet\left[C_n(\mathbf{v}-w^s\mathbf{e}_z)-\mathbf{K}\bullet\nabla C_n\right] \tag{107}$$

The bottom boundary conditions must account for erosion or deposition rates: see, e.g., equations (4) and (5) of Gong and Shen (2010). On another note, we can use a similar equation for other types of sinking particles such as, for example, diatoms (e.g., Deleersnijder et al. 2006).

In estuaries and coastal regions, wetting and drying (essentially due to tides) is a crucial phenomenon. Representing its impact in the water and momentum conservation equations is still a significant challenge for numerical modellers (e.g., Balzano 1998, Gourgue et al. 2009, Kärnä et al. 2011, Medeiros and Hagen 2013, Vater et al. 2015, Li and Zhang 2021, Ortleb et al. 2022). Rightly or wrongly, the corresponding treatment of the reactive transport equations is often considered more straightforward.

Today's numerical models of environmental fluid flows and the associated reactive transport processes, and, to a lesser degree, field data collection systems produce vast amounts of real numbers. Making sense of them, i.e., identifying key processes and establishing causal relationships between them, is no trivial task. Analysing primitive variables (velocity components, pressure, temperature, concentrations, etc.) is not always conducive to the most fruitful interpretations (see, e.g., Lucas and Deleersnijder 2020 and references therein). An option worth considering consists in examining auxiliary variables,

e.g., local effective diffusivities estimated *a posteriori* (Petton et al. 2020) or timescales such as the age or the residence/exposure time, introduced for diagnostic purposes (see, e.g., Deleersnijder et al. 2018, Lucas and Deleersnijder 2020 and references therein). Such variables may also be instrumental in designing reduced-dimension models, which may be used as interpretation or simplified prediction tools (see, e.g., Deleersnijder et al. 1998, Deleersnijder 2009, Lucas et al. 2009b, Lucas and Thompson 2012, Mouchet et al. 2012, Lucas and Deleersnijder 2020 and references therein, Shen et al. 2022). Novel diagnostic timescale concepts are under development (e.g., Delhez and Wolk 2013, Mouchet et al. 2016, Gross et al. 2019, Lin and Liu 2019, Dewals et al. 2020, Deleersnijder 2020b, 2021).

Acknowledgements. Over the past decade, ED had thought-provoking discussions with Benoît Cushman-Roisin, Anouk de Brauwere, Eric J.M. Delhez, Benjamin Dewals, Edward Gross, Arnold W. Heemink, Lisa V. Lucas, Arjen Markus, Anne Mouchet and Henk M. Schuttelaars. These exchanges of views indirectly helped prepare the present working note.

References

Balzano A., 1998, Evaluation of methods for numerical simulation of setting and drying in shallow water flow models, *Coastal Engineering*, 34, 83-107

Baretta-Bekker H.J.G., E.K. Duursma and B.R. Kuipers (editors), 1998, *Encyclopedia of Marine Sciences*, Springer, Berlin, 357 pages

Batchelor G.K., 1967, *An Introduction to Fluid Dynamics*, Cambridge University Press, 615 pages

Batchelor G.K. and A.A. Townsend, 1956, Turbulent diffusion, in: G.K. Batchelor and R.M. Davies (editors), *Surveys in Mechanics*, Cambridge University Press, pages 352-399

Baumert H.Z., J.H. Simpson and J. Sündermann (editors), 2005, *Marine Turbulence: Theories, Observations and Models – Results of the CARTUM Project*, Cambridge University Press, 630 pages

Beckers J.-M., H. Burchard, J.-M. Campin, E. Deleersnijder and P.-P. Mathieu, 1998, Another reason why simple discretisations of rotated diffusion operators cause problems in ocean models: comments on "Isoneutral diffusion in a z-coordinate ocean model", *Journal of Physical Oceanography*, 28, 1552-1559

Bedford K.W., J.S. Dingman and W.K. Yeo, 1987, Preparation of estuary and marine models equations by generalized filtering methods, in: J.C.J. Nihoul and B.M. Jamart (editors), *Three-dimensional Models of Marine and Estuarine Dynamics*, Elsevier, Amsterdam, pages113-125

Blaise S. and E. Deleersnijder, 2008, Improving the parameterisation of horizontal density gradient in one-dimensional water column models for estuarine circulation, *Ocean Science*, 4, 239-246

Blumberg A.F. and G. L. Mellor, 1987, A description of a three-dimensional coastal ocean

circulation model, in: N.S. Heaps (editor), *Three Dimensional Coastal Models*, American Geophysical Union, Washington, D.C., pages 1-16

Boussinesq J., 1877, Essai sur la théorie des eaux courantes, *Mémoires Présentés par divers Savants à l'Académie des Sciences*, 23(1), 1-680

Burchard H., 2002, *Applied Turbulence Modelling in Marine Waters*, Lectures Notes in Earth Science, No. 100, Springer, Heidelberg, 215 pages

Burchard H., E. Deleersnijder and A. Meister, 2003, A high-order conservative Patankar-type discretisation for stiff systems of production-destruction equations, *Applied Numerical Mathematics*, 47, 1-30

Campin J.-M., C. Hill, H. Jones and J. Marshall, 2011, Super-parameterization in ocean modelling: Application to deep convection, *Ocean Modelling*, 36, 90-101

Canuto V.M., A.M. Howard, Y. Cheng, C.J. Muller, A. Leboissetier and S.R. Jayne, 2010, Ocean turbulence, III: New GISS vertical mixing scheme, *Ocean Modelling*, 34, 70-91

Chavez E.W.V., 2013, *Notes on Continuum Mechanics*, in: Lecture Notes on Numerical Merthods in Engineering and Sciences, Springer, Dordrecht, Netherlands, 673 pages

Crossland C.J., D. Baird, J.-P. Ducrotoy, H. Lindeboom, R.W. Buddemeier, W.C. Dennison, B.A. Maxwell, S.V. Smith and D.P.Swaney, 2005, The coastal zone - A domain of global interactions. in: C.J. Crossland, H.H. Kremer, H.J. Lindeboom, J.I. Marshall, and M.D.A. Tissier (editors), *Coastal Fluxes in the Anthropocene*, Springer, Berlin, pages 1- 37

Cushman-Roisin B., 1989, *A flavour of Mesoscale Physical Oceanography*, IBM BSC 89/3, IBM Bergen Scientific Centre, Bergen, Norway, 78 pages

Cushman-Roisin B., 2008, Beyond eddy diffusivity: an alternative model for turbulent dispersion, *Environmental Fluid Mechanics*, 8, 543-549

Cushman-Roisin B., 2022, Turbulent dispersion, in: *The Mathematics of Marine Modelling – Water, Solute and Particle Dynamics in Estuaries and Shallow Seas*, H. Schuttelaars, A. Heemink and E. Deleersnijder (editors), Mathematics of Planet Earth 9, Springer Nature, Cham, Switzerland, pages 167-196

Cushman-Roisin B. and J.-M. Beckers, 2011 (2nd ed.), *Introduction to Geophysical Fluid Dynamics - Physical and Numerical Aspects*, Elsevier, Amsterdam, 828 pages

Davenport E.D., C. Fan, J.J. Govoni and J. Anderson, 2012, Description and application of a NPZD model to forecast hurricane impacts to secondary production in coastal ecosystems, *Procedia Environmental Sciences*, 13, 1569-1584

de Brauwere A., N. Koffi Ouattara and P. Servais, 2014, Modeling fecal indicator bacteria concentration in natural surface waters: a review, *Critical Reviews in Environmental Science and Technology*, 44, 2380-2453

de Brye B., A. de Brauwere, O. Gourgue, E.J.M. Delhez and E. Deleersnijder, 2012, Water renewal timescales in the Scheldt Estuary, *Journal of Marine Systems*, 94, 74-86

de Groot S.R. and P. Mazur, 1962, *Non-Equilibrium Thermodynamics*, North-Holland, Amsterdam, 510 pages

Dee D.P., 1995, A pragmatic approach to model validation, in: *Quantitative Skill Assessment for Coastal Ocean Models*, D.R. Lynch and A.M. Davies (editors), Coastal and Estuarine Studies, Volume 47, American Geophysical Union, Washington, DC, pages 1-13

Delandmeter P., J. Lambrechts, V. Legat, V. Vallaeys, J. Naithani, W. Thiery, J.-F. Remacle and E. Deleersnijder, 2018, A fully consistent and conservative vertically adaptive coordinate system for SLIM 3D v0.4 with an application to the thermocline oscillations of Lake Tanganyika, *Geoscientific Model Development*, 11, 1161-1179

Deleersnijder E., 2007, *Analytical solutions to assess Lagrangian models of advective and diffusive transport processes*, Working note, Université catholique de Louvain, Louvain-la-Neuve, 24 pages, available on the web at URL http://hdl.handle.net/2078.1/155421

Deleersnijder E., 2009, *The unreasonable effectiveness of dimension reduction in complex geophysical flow modelling*, Working note, Université catholique de Louvain, Louvain-la-Neuve, 24 pages, available on the web at URL http://hdl.handle.net/2078.1/154174

Deleersnijder E., 2011, Test cases for advection-diffusion equations with a first-order decay term, Working note, Université catholique de Louvain, Louvain-la-Neuve, 23 pages, available on the web at URL http://hdl.handle.net/2078.1/155372

Deleersnijder E., 2012, *Homogenisation of a passive tracer concentration in an isolated domain*, Working Note, Université catholique de Louvain, Louvain-la-Neuve, Belgium, 7 pages, available on the web at URL http://hdl.handle.net/2078.1/155297

Deleersnijder E., 2014, *On the structure of a compartment model for tracer transport*, Working Note, Université catholique de Louvain, Louvain-la-Neuve, Belgium, 7 pages, available on the web at URL http://hdl.handle.net/2078.1/155581

Deleersnijder E., 2019a, *A note on the estimation of orders of magnitude in marine sciences*, Working Note, Université catholique de Louvain, Louvain-la-Neuve, Belgium, 3 pages, available on the web at URL http://hdl.handle.net/2078.1/221004

Deleersnijder E., 2019b, *A shortcoming of Fourier-Fick parameterisations in turbulent flows*, Working Note, Université catholique de Louvain, Louvain-la-Neuve, Belgium, 4 pages, available on the web at URL http://hdl.handle.net/2078.1/222453

Deleersnijder E., 2019c, *From Leibniz integral rule to Reynolds' transport theorem*, Université catholique de Louvain, Louvain-la-Neuve, Belgium, 6 pages, available on the web at URL http://hdl.handle.net/2078.1/221577

Deleersnijder E., 2019d, *Water renewal of a region of freshwater influence (ROFI): mathematical properties of some of the relevant diagnostic variables*, Université catholique de Louvain, Louvain-la-Neuve, Belgium, 19 pages, available on the web at URL http://hdl.handle.net/2078.1/220841

Deleersnijder E., 2020a, *The uneasy collaboration of Leonhard Euler (1707-1783) and Joseph Louis de Lagrange (1736-1813) in environmental fluid mechanics*, Université catholique de Louvain, Louvain-la-Neuve, Belgium, 5 pages, available on the web at URL http://hdl.handle.net/2078.1/229071

Deleersnijder E., 2020b, *An attempt at defining a position-dependent flushing time*, Université

catholique de Louvain, Louvain-la-Neuve, Belgium, 14 pages, available on the web at URL http://hdl.handle.net/2078.1/231030

Deleersnijder E., 2021, *On the method for estimating the mean property experienced by a tracer pioneered by Gross et al. (2019)*, Université catholique de Louvain, Louvain-la-Neuve, Belgium, 30 pages, available on the web at URL http://hdl.handle.net/2078.1/247973

Deleersnijder E., J.-M. Beckers and E.J.M. Delhez, 2006, The residence time of settling particles in the surface mixed layer, *Environmental Fluid Mechanics*, 6, 25-42

Deleersnijder E., A. Mouchet and E.J.M. Delhez, 2018, *Diagnostic timescales in fluid flows: from the Tower of Babel to partial differential equations*, Working note, Université catholique de Louvain, Louvain-la-Neuve, Belgium, 26 pages, available on the web at URL http://hdl.handle.net/2078.1/196273

Deleersnijder E., J. Wang and C.N.K. Mooers, 1998, A two-compartment model for understanding the simulated three-dimensional circulation in Prince William Sound, Alaska, *Continental Shelf Research*, 18, 279-287

Deleersnijder E. and E. Wolanski, 1990, Du rôle de la dispersion horizontale de quantité de mouvement dans les modèles marins tridimensionnels, in: Proceedings of the *"Journées Numériques de Besançon - Courants Océaniques"*, J.-M. Crolet and P. Lesaint (eds.), Publications mathématiques de Besançon, pages 39-50, available on the web at URL https://hdl.handle.net/2268/305714

Dewals B., P. Archambeau, M. Bruwier, S. Erpicum, M. Pirotton, T. Adam, E. Delhez and E. Deleersnijder, 2020, Age of water particles as a diagnosis of steady-state flows in shallow rectangular reservoirs, *Water*, 12, 2819, doi: 10.3390/w12102819

Dickey T.D., 2003, Emerging ocean observations for interdisciplinary data assimilation systems, *Journal of Marine Systems*, 40-41, 5-48

Duquesne F., V. Vallaeys, P. Jai Vidaurre and E. Hanert, 2021, A coupled ecohydrodynamic model to predict algal blooms in Lake Titicaca, *Ecological Modelling*, 440, 109418, doi: 10.1016/j.ecolmodel.2020.109418

Elskens M., O. Gourgue, W. Baeyens, L. Chou, E. Deleersnijder, M. Leermakers and A. de Brauwere, 2014, Modelling metal speciation in the Scheldt Estuary: combining a flexible-resolution transport model with empirical functions, *Science of the Total Environment*, 476-477, 346-358

Fasham M.J.R., H.W. Ducklow and S.M. McKelvie, 1990, A nitrogen based model of plankton dynamics in the oceanic mixed layer, *Journal of Marine Research*, 48, 591-639

Feistel R., 2008, A Gibbs function for seawater thermodynamics for -6 to 80 °C and salinity up to 120 g kg^{-1}, *Deep Sea Research I*, 55, 1639-1671

Ferziger J., 2005, Turbulence: its origins and structure, in: H.Z. Baumert, J.H. Simpson and J. Sündermann (editors), *Marine Turbulence: Theories, Observations and Models - Results of the CARTUM Project*, Cambridge University Press, pages 4-13

Fick A., 1885, Über Diffusion, *Annalen der Physik*, 170, 59-86

Fischer H.B., E. J. List, R.C.Y Koh, J. Imberger and N.H. Brooks, 1979, *Mixing in Inland and Coastal Waters*, Academic Press, San Diego, 483 pages

Fringer O.B., C.N. Dawson, R. He, D.K. Ralston and Y.J. Zhang, 2019, The future of coastal and estuarine modeling: Findings from a workshop, *Ocean Modelling*, 143, 101458, doi: 10.1016/j.ocemod.2019.101458

Frisch U., 1995, *Turbulence*, Cambridge University Press, 296 pages

Garabedian P., 1964, Partial Differential Equations, Chelsea Publishing Company, New York, 672 pages

Gerdes R., 1993, A primitive equation ocean circulation model using a general vertical coordinate transformation 1. Description and testing of the model, *Journal of Geophysical Research*, 98, 14683-14701

Germano M., 1992, Turbulence: the filtering approach, *Journal of Fluid Mechanics*, 238, 325-3336

Gong W. and J. Shen, 2010, A model diagnostic study of age of river-borne sediment transport in the tidal York River Estuary, *Environmental Fluid Mechanics*, 10, 177-196

Gourgue O., W. Baeyens, M.S. Chen, A. de Brauwere, B. de Brye, E. Deleersnijder, M. Elskens and V. Legat, 2013, A depth-averaged two-dimensional sediment transport model for environmental studies in the Scheldt Estuary and tidal river network, *Journal of Marine Systems*, 128, 27-39

Gourgue O., R. Comblen, J. Lambrechts, T. Kärnä, V. Legat and E. Deleersnijder, 2009, A flux-limiting wetting-drying method for finite-element shallow-water models, with an application to the Scheldt Estuary, *Advances in Water Resources*, 32, 1726-1739

Gräwe U., E. Deleersnijder, S.H.A.M. Shah and A.W. Heemink, 2012, Why the Euler-scheme in particle-tracking is not enough: the shallow-sea pycnocline test case, *Ocean Dynamics*, 62, 501-514

Gross E., S. Andrews, B. Bergamashi, B. Downing, R. Holleman, S. Burdick and J. Durand, 2019, The use of stable isotope-based water age to evaluated a hydrodynamic model, *Water*, 11, 2207, doi: 10.3390/w11112207

Gross E., R. Holleman, W. Kimmerer, S. Munger, S. Burdick and J. Durand, 2023, Using age tracers to estimate ecological rates in a phytoplankton model, *Water*, 15, 2097, doi: 10.3390/w15112097

Groβe F., K. Fennel and A. Laurent, 2019, Quantifying the relative importance of riverine and open-ocean nitrogen sources for hypoxia formation in the northern Gulf of Mexico, *Journal of Geophysical Research: Oceans*, 124, 5451-5467, doi: 10.1029/2019JC015230

Hannah W.M., C.R Jones, B.R. Hillman, M.R. Norman, D.C. Bader, M.A. Taylor, L.R. Leung, M.S. Pritchard, M.D. Branson, G. Link, K.G. Pressel and J.M. Lee, 2020, Initial results from the super-parameterized E3SM, *Journal of Advances in Modeling Earth Systems*, 12, e2019MS001863

Heinle A. and T. Slawig, 2013, Internal dynamics of NPZD type ecosystem models, *Ecological Modelling*, 254, 33-42

Jähne B. and H. Hauβecker, 1998, Air-water gas exchange, *Annual Review of Fluid Mechanics*, 30, 443-468

Jou D., J. Casas-Vasquez and G. Lebon, 1996, *Extended Irreversible Thermodynamics*, Springer, Berlin, 383 pages

Hirt C.W., A.A. Amsden and J.L. Cook, 1974, An arbitrary Lagrangian-Eulerian computing method for all flow speeds, *Journal of Computational Physics*, 14, 227-253

Kärnä T., B. de Brye, O. Gourgue, J. Lambrechts, R. Comblen, V. Legat and E. Deleersnijder, A fully implicit wetting-drying method for DG-FEM shallow water models, with an application to the Scheldt Estuary, *Computer Methods in Applied Mechanics and Engineering*, 200, 509-524

Kopecz S. and A. Meister, 2019, On the existence of three-stage third-order modified Patankar-Runge-Kutta schemes, *Numerical Algorithms*, 81, 1473-1484

Kundu P.K., I.M. Cohen and D.R. Dowling, 2012 (5th ed.), *Fluid Mechanics*, Academic Press, 891 pages

Lacroix G. and P. Nival, 1998, Influence of meteorological variability on primary production dynamics in the Ligurian Sea (NW Mediterranean Sea) with a 1D hydrodynamic/biological model, *Journal of Marine Systems*, 16, 23-50

Large W.G., J.C. McWilliams and S.C. Downey, 1994, Oceanic vertical mixing: a review and a model with a nonlocal boundary layer parameterization, *Reviews of Geophysics*, 32, 363-403

Lasaga A.C., The kinetic treatment of geochemical cycles, *Geochimica et Cosmochimica Acta*, 44, 815-828

Legrand S., E. Deleersnijder, E. Hanert, V. Legat and E. Wolanski, 2006, High-resolution, unstructured meshes for hydrodynamic models of the Great Barrier Reef, Australia, *Estuarine, Coastal and Shelf Science*, 68, 36-46

Lewandowski R., 1997, *Analyse Mathématique et Océanographie*, Masson, Paris, 281 pages

Li L. and Q. Zhang, 2021, Development of an efficient wetting and drying treatment for shallo-water modeling using the quadrature-free Runge-Kutta discontinuous Galerkin method, *International Journal for Numerical Methods in Fluids*, 93, 314-338

Lighthill J., 1978, *Waves in Fluids*, Cambridge University Press, 504 pages

Lin L. and Z. Liu, 2019, Partial residence times: determining residence time composition in different subregions, *Ocean Dynamics*, 69, 1023-1036

Lucas L.V. and E. Deleersnijder, 2020, Timescale methods for simplifying, understanding and modeling biophysical and water quality processes in coastal aquatic ecosystems: a review, *Water*, 12, 2717, doi: 10.3390/w12102717

Lucas L.V., J.R. Koseff, S.G. Monismith and J.K. Thompson, 2009a, Shallow water processes govern system-wide phytoplankton bloom dynamics: a modeling study, *Journal of Marine Systems*, 75, 70-86

Lucas L.V. and J.K. Thompson, 2012, Changing restoration rules: exotic bivalves interact

with residence and depth to control phytoplankton productivity, *Ecosphere*, 3, 117, doi: 10.1890/ES12-00251.1

Lucas L.V., J.K. Thompson and L.R. Brown, 2009b, Why are diverse relationships observed between phytoplankton biomass and transport time, *Limnology and Oceanography*, 54, 381-390

Lynch D.R. and A.M. Davies (editors), 1995, *Quantitative Skill Assessment for Coastal Ocean Models*, Coastal and Estuarine Studies, Volume 47, American Geophysical Union, Washington, DC, 510 pages

Marshall J., C. Hill, L. Perelman and A. Adcroft, 1997, Hydrostatic, quasi-hydrostatic, and nonhydrostatic ocean modeling, *Journal of Geophysical Research (Oceans)*, 102, 5733-5752

Mata Almonacid P. and C. Medel, 2022, A structure-preserving model for the dynamics of estuarine ecosystems and its application in western Patagonia fjords, *Ecological Modelling*, 466, 109871, doi: 10.1016/j.ecolmodel.2021.109871

Medeiros S.C. and S.C. Hagen, 2013, Review of wetting and drying algorithms for numerical tidal flow models, *International Journal for Numerical Methods in Fluids*, 71, 473-487

Mellor G.L. and A.F. Blumberg, 1985, Modeling vertical and horizontal diffusivities with the sigma coordinate system, *Monthly Weather Review*, 113, 1379-1383

Mellor G.L. and T. Yamada, 1982, Development of a tubulence closure model for geophysical fluid problems, *Reviews of Geophysics and Space Physics*, 20, 851-875

Moll A. and G. Radach, 2003, Review of three-dimensional ecological modelling related to the North Sea shelf system - Part 1: models and their results, *Progress in Oceanography*, 57, 175-217

Mouchet A., 2013, The ocean bomb radiocarbon inventory revisited, *Radiocarbon*, 55, 1580-1594

Mouchet A., F. Cornaton, E. Deleersnijder and E.J.M. Delhez, 2016, Partial ages: diagnosing transport processes by means of multiple clocks, *Ocean Dynamics*, 66, 367-386

Naithani J., B. de Brye, E. Buyze, W. Vyverman, V. Legat and E. Deleersnijder, 2016, An ecological model for the Scheldt estuary and tidal river ecosystem: spatial and temporal variability of plankton, *Hydrobiologia*, 775, 51-67

Naithani J., P.-D. Plisnier and E. Deleersnijder, 2011, Possible effects of global climate change on the ecosystem of Lake Tanganyika, *Hydrobiologia*, 671, 147-163

Nihoul J.C.J., 1981, *Basic Equations of Geophysical Fluid Dynamics and their Application to Ocean-Atmosphere Weather and Climate Models*, Belgian visiting professorhip 1980-1981, Department of Mathematics, Imperial College, London, 61 pages, available on the web at URL http://hdl.handle.net/2268/240525

Nihoul J.C.J., 1993, Application of mathematical modeling to the marine environment, in: P. Zanetti (Ed.), *Environmental Modeling*, Vol I, Elsevier, pages 75-140

Okubo A., 1971, Oceanic diffusion diagrams, *Deep-Sea Research*, 18, 789-802

Okubo A., 1976, Remarks on the use of 'diffusion diagrams' in modeling scale-dependent diffusion, *Deep-Sea Research*, 23, 1213-1214

Oreskes N., K. Shrader-Frechette and K. Belitz, 1994, Verification, validation, and confirmation of numerical models in the Earth sciences, *Science*, 263, 641-646

Ortleb S., J. Lambrechts and T. Kärnä, 2022, Wetting and drying procedures for shallow water simulations, in: *The Mathematics of Marine Modelling – Water, Solute and Particle Dynamics in Estuaries and Shallow Seas*, H. Schuttelaars, A. Heemink and E. Deleersnijder (editors), Mathematics of Planet Earth 9, Springer Nature, Cham, Switzerland, pages 287-314

Petton S., S. Pouvreau and F. Dumas, 2020, Intensive use of Lagrangian trajectories to quantify coastal area dispersion, *Ocean Dynamics*, 70, 541-559

Radtke H., T. Neumann, M. Voss and W. Fennel, 2012, Modeling pathways of riverine nitrogen and phosphorus in the Baltic Sea, *Journal of Geophysical Research*, 117, C09024, doi: 10.1029/2012JC008119

Raick C., A. Alvera-Azcarate, A. Barth, J.M. Brankart, K. Soetaert and M. Grégoire, 2007, Application of a SEEK filter to a 1D biogeochemical model of the Ligurian Sea: twin experiments and real in-situ data assimilation, *Journal of Marine Systems*, 65, 561-583

Raillard O. and A. Ménesguen, 1994, An ecosystem box model for estimating the carrying capacity of a macrotidal shellfish sytem, *Marine Ecology Progress Series*, 115, 117-130

Rao Y.R., C.R. Murthy and P.C. Sinha, 2008, The coastal ocean, in: C.R. Murthy, P.C. Sinha and Y.R. Rao (editors), *Modelling and Monitoring of Coastal Marine Processes*, Springer, Dordrecht, pages 3-10

Reynolds O., 1883, An experimental investigation of the circumstances which determine whether the motion of water shall be direct or sinuous, and of the law of resistance in parallel channels, *Philosophical Transactions of the Royal Society of London*, 174, 935-982

Reynolds O., 1895, On the dynamical theory of incompressible viscous fluids and the determination of the criterion, *Philosophical Transactions of the Royal Society of London A*, 186, 123-164

Roache P.J., 1982, *Computational Fluid Dynamics*, Hermosa Publishers, Albuquerque, 446 pages

Rodi W., 1993, *Turbulence Models and their Applications in Hydraulics — A State-of-the-Art Review*, IAHR-AIRH Monograph (3rd edn.), A.A. Balkema, Rotterdam, 104 pages

Rutherford J.C., 1994, *River Mixing*, Wiley, Chichester, England, 347 pages

Schuchert P., L. Kregting, D. Pritchard, G. Savidge and B. Elsäβer, 2018, Using coupled hydrodynamic biogeochamical models to predict the effects of tidal turbine arrays on phytoplankton dynamics, *Journal of Marine Science and Engineering*, 6, 58, doi: 10.3390/jmse6020058

Shapiro G., M. Luneva, J. Pickering and D. Storkey, 2013, The effect of various vertical discretization schemes and horizontal diffusion parameterization on the performance of a

3-D ocean model: the Black Sea case study, *Ocean Science*, 9, 377-390

Shen J., J. Du and L.V. Lucas, 2022, Simple relationships between residence time and annual nutrient retention, export, and loading for estuaries, *Limnology and Oceanography*, 67, 918-933

Silverman B.W., 1986, *Density Estimation for Statistics and Data Analysis*, Chapman & Hall, London, 175 pages

Smagorinsky J., 1963, General circulation experiments with the primitive equations. I. The basic experiment, *Monthly Weather Review*, 91, 99-164

Spivakovskaya D., A.W. Heemink and E. Deleersnijder, 2007a, Lagrangian modelling of multi-dimensional advection-diffusion with space-varying diffusivities: theory and idealized tests cases, *Ocean Dynamics*, 57, 189-203

Spivakovskaya D., A.W. Heemink and E. Deleersnijder, 2007b, The backward Ito method for the Lagrangian simulation of transport processes with large space variations of the diffusivity, *Ocean Science*, 3, 525-535

Stijnen J.W., A.W. Heemink and H.X. Lin, 2006, An efficient 3D particle transport model for use in stratified flow, *International Journal for Numerical Methods in Fluids*, 51, 331-350

Stull R.B., 1988, *An Introduction to Boundary Layer Meteorology*, Kluwer Academic Publishers, Dordrecht, Netherlands, 666 pages

Taylor K.E., 2001, Summarizing multiples aspects of model performance in a single diagram, *Journal of Geophysical Research*, 106, 7183-7192

Thuburn J., 1997, TVD schemes, positive schemes, and the universal limiter, *Monthly Weather Review*, 125, 1990-1993

Umlauf L. and H. Burchard, 2003, A generic length-scale equation for geophysical turbulence models, *Journal of Marine Research*, 61, 235-265

Umlauf L. and H. Burchard, 2005, Second-order turbulence closure models for geophysical boundary layers. A review of recent work, *Continental Shelf Research*, 25, 795-827

Vallaeys V., T. Kärnä, P. Delandmeter, J. Lambrechts, A.M. Baptista, E. Deleersnijder and E. Hanert, 2018, *Ocean Modelling*, 124, 111-124

van Sebille E., S.M. Griffies, R. Abernathey, T.P. Adams, P. Berloff, A. Biastoch, B. Blanke, E.P. Chassignet, Y. Cheng, C.J. Cotter, E. Deleersnijder, K. Döös, H. Drake, S. Drijfhout, S.F. Gary, A.W. Heemink, J. Kjellsson, I.M. Koszalka, M. Lange, C. Lique, G.A. MacGilchrist, R. Marsh, C.G. Mayorga Adame, R. McAdam, F. Nencioli, C.B. Paris, M.D. Piggott, J.A. Polton, S. Rühs, S.H.A.M. Shah, M.D. Thomas, J. Wang, P.J. Wolfram, L. Zanna and J.D. Zika, 2018, Lagrangian ocean analysis: fundamentals and practices, *Ocean Modelling*, 121, 49-75

Vater S., N. Beisiegel and J. Behrens, 2015, A limiter-based well-balanced discontinuous Galerkin method for shallow-water flows with wetting and drying: one-dimensional case, *Advances in Water Resources*, 85, 1-13

Vaz A.C., M. Karnauskas, C.B. Paris, J.C. Doerrs, R.L. Hill, C. Horn, M.H. Miller, M. Neuman, K.J. McCarthy and N.A. Farmer, 2022, Exploitation drives changes in the

population connectivity of queen conch (*Aliger gigas*), *Frontiers in Marine Science*, 9, 841027, doi: 10.3389/fmars.2022.841027

von Storch H., 2001, Models between academia and applications, in: H. von Storch and G. Flöser (editors), *Models in Environmental Research*, Springer, Berlin, pages 17-33

Wang J., Y.M. Dijkstra and H.E. de Swart, 2022, Turbidity maxima in estuarine networks: dependence on fluvial sediment input and local deepening/narrowing with an exploratory model, *Frontiers in Marine Science*, 9, 940081, doi: 10.3389/fmars.2022.940081

Wanninkhof R., 1992, Relationship between speed and gas exchange over the ocean, *Journal of Geophysical Research*, 97 (C5), 7373-7382

Warner J.C., W.R. Geyer and J.A. Lerczak, 2005a, Numerical modeling of an estuary: a comprehensive skill assessment, *Journal of Geophysical Research*, 110, C05001, doi: 10.1029/2004JC002691

Warner J.C., C.R. Sherwood, H.G. Arango and R.P. Signell, 2005b, Performance of four turbulence closure models implemented using a generic legth scale method, *Ocean Modelling,* 8, 81-113

Welander P., 1955, Studies on the general development of motion in a two-dimensional, ideal fluid, *Tellus*, 7, 141-156

White L., V. Legat and E. Deleersnijder, 2008, Tracer conservation for thee-dimensional, finite-element, free-surface, ocean modeling on moving prismatic meshes, *Monthly Weather Review*, 136, 420-442

Willmott C.J., 1981, On the validation of models, *Physical Geography*, 2, 184-194

Wolanski E., R. Brinkman, S. Spagnol, F. McAllister, C. Steinberg, W. Skirving and E. Deleersnijder, 2003, Merging scales in models of water circulation: perspectives from the Great Barrier Reef, in: *Advances in Coastal Modeling*, V.C. Lakhan (Ed.), Elsevier, pp. 411-429

Xiong J. and J. Shen, 2022, Vertical transport timescale of surface-produced particulate material in the Chesapeake Bay, *Journal of Geophysical Research: Oceans*, 127, e2021JC017592, doi: 10.1029/2021JC017592

Yool A. and M.J. Fasham, 2001, An examination of the "continental shelf pump" in an open ocean general circulation model, *Global Biogeochemical Cycles*, 15, 831-844
